



Operations on Complex Neutrosophic Soft Sets and Their Topological Spaces: A New Approach with Applications to Decision-Making

A. A. Azzam¹, Alaa M. Abd El-latif², B. Alreshidi¹, M. Aldawood¹,
Mohamed M. Awad¹, Hamza Ali Abujabal³, Cris L. Armada^{4,5}, Arif Mehmood^{6,*}

¹ Department of Mathematics, Faculty of Science and Humanities, Prince Sattam Bin Abdulaziz University, Al-Kharj 11942, Saudi Arabia

² Department of Mathematics, College of Science, Northern Border University, Arar 91431, Saudi Arabia

³ Department of Mathematics, King Abdulaziz University, P.O. Box 80003, Jeddah 21589, Saudi Arabia

⁴ National University Ho Chi Minh City, Linh Trung Ward, Thu Duc City, Ho Chi Minh City, Vietnam

⁵ Department of Applied Mathematics, Faculty of Applied Science, Ho Chi Minh City University of Technology (HCMUT), 268 Ly Thuong Kiet, Ward 14, District 10, Ho Chi Minh City, Vietnam

⁶ Department of Mathematics, Institute of Numerical Sciences, Gomal University, Dera Ismail Khan 29050, KPK, Pakistan

Abstract. This research presents a new theoretical framework and shows how to use it effectively to data analysis. First, we introduce a novel method to complex neutrosophic soft sets (CNSS) and ensure the generalize ability of their use by defining basic operations such as union, intersection, and complement. We go on to construct a complete one-value neutrosophic soft topology, defining the most important topological properties such as interior, closure, and other related theoretical aspects, to give a strong mathematical foundation. An example is then provided to illustrate this framework's analytical capabilities. Using a comprehensive visualizing package that includes spline-smoothed functional curves, 3D surface plots, and 2D Heatmaps, we apply our method to address a signal-template alignment problem. The Cotangent Similarity Measure (Cot SM) is used to systematically examine three input signals ($S_1 - S_3$) and three templates ($T_1 - T_3$). The findings are striking and unambiguous: a worldwide maximum indicates a high degree of confidence, and the correlation between $S_2 - T_1$ ($CotSM = 0.6653$) is widely recognized as the strongest and most conclusive connection. Subsequent analysis shows that while signal S_2 is the most important overall, signals S_1 and S_3 are helpful for particular targets.

2020 Mathematics Subject Classifications: 03E72, 54A40, 68T10, 62H30

Key Words and Phrases: Complex neutrosophic soft sets, complex neutrosophic soft topology, cotangent similarity measures, data visualization techniques

1. Introduction

Zadeh's invention of fuzzy sets [1] revolutionized mathematical modeling of uncertainty by introducing a graded membership (degree) in place of the binary membership of a classical set theory. This fundamental idea allowed machines to handle human reasoning's imprecision,

*Corresponding author.

DOI: <https://doi.org/10.29020/nybg.ejpam.v18i4.7171>

Email addresses: aa.azzam@psau.edu.sa (A. A. Azzam), alaa.ali@nbu.edu.sa (A. M. Abd El-latif), b.alreshidi@psau.edu.sa (B. Alreshidi), m.aldawood@psau.edu.sa (M. Aldawood), m.abdelgalil@psau.edu.sa (M. M. Awad), haabujabal@kau.edu.sa (H. A. Abujabal), cris.armada@hcmut.edu.vn (C. L. Armada), mehdaniyal@gmail.com (A. Mehmood)

leading to the development of entire fields like fuzzy logic. However, the intricacy of the issues made it impossible to combine all available data into a single membership level, which was the constraint. Complex Fuzzy Sets (CFSs), where the membership is a complex number, were first introduced by Ramot et al. [2] as a solution to this problem. Both amplitude (the traditional membership grade) and phase term (coding additional, typically cyclic, data) are represented in this model. Studies that integrated the complex structure with other advanced fuzzy structures were revived as a result of this breakthrough, which added a complex element to the uncertainty representation. A hybrid super model family was created as a result of this combination. Alkouri and Salleh developed Complex Intuitionistic Fuzzy Sets (CIFSs) to represent complex-valued membership and non-membership in order to offer a more thorough account of hesitation [3]. Complex Neutrosophic Sets (CNSs), a potent theory based on complex numbers that conveys truth, indeterminacy, and falsity memberships independently, were later proposed by Ali and Smarandache [4]. In order to address imprecision even in complex memberships, this was further developed to Interval Complex Neutrosophic Sets (ICNSs) [5]. At the same time, a great deal of research has improved these models' theoretical foundation. Garg and Rani studied the aggregation operators of Complex Interval-Valued Intuitionistic Fuzzy Sets [7], whereas Al-Qudah and Hassan studied the functions of Complex Multi-Fuzzy Sets [6]. In the event that there are several possible complex evaluations, Garg et al. later presented Complex Hesitant Fuzzy Sets, which include additional distance measures [8]. Singh constructed a concept lattice using Complex Vague Sets to illustrate the versatility of these ideas [9]. Scientists have expanded their conceptual richness and applicability based on the basic frameworks of complicated neutrosophic sets. Its ability to capture both the positive and negative memberships of truth and indeterminacy and falsity in the complex plane makes it a significant extension, first presented by RaBroumi et al. as Bipolar Complex Neutrosophic Sets [10]. As a result, it is a more effective tool for use in decision-making problems where opposing factors are present.

Al-Quran and Alkhazaleh studied the significance of the relations between complicated neutrosophic sets [12], and Quek et al. [11] constructed the sets in the theoretical framework of graph theory. Linguistic solutions to interval complicated neutrosophic sets were provided by Dat et al. [13] to bridge the gap between the numerical and linguistic representations, making them more useful in human-based decision-making scenarios. Molodtsov introduced Soft Set Theory, another similarly potent paradigm for handling uncertainty, at the same time [14].

This gave a totally new, parameterized manner of treating imprecision that was not subject to the limits of the old-fashioned membership functions. The combination of pre-existing fuzzy models and soft sets quickly became a productive area of study. Maji et al. made the initial attempt at this synergy when they launched fuzzy soft sets [15] and intuitionistic fuzzy soft sets [16], which parameterized soft sets but with fuzzy and intuitionistic fuzzy set capability, respectively. This trend of hybridization continued to embrace increasingly intricate forms of uncertainty. The researchers that had to deal with uncertain membership information developed Interval-Valued Fuzzy Soft Sets [17] and Interval-Valued Intuitionistic Fuzzy Soft Sets [18]. Moreover, neutrosophic theory was adopted with the introduction of Neutrosophic Soft Sets by Maji [19] and Interval-Valued Neutrosophic Soft Sets by Deli [22]. These two unconnected concepts describe the truth, indeterminacy, and falsity of parameters separately.

Abu Qamar and Hassan's [23] introduction of the Q-Neutrosophic Soft Set, which demonstrates the contemporary and dynamic intersection of complex, neutrosophic, and soft set theories to handle the complexity of uncertainty in data, is one of the even more extended forms of the area that are now being explored. More sophisticated and specialized models have been produced as a result of the ongoing hybridization trend. By studying the algebraic structures of Q-neutrosophic soft fields, Abu Qamar et al. developed the theoretical foundation of the study and further formalized the work on Q-Neutrosophic Soft Sets [24]. The model's ability to progress from pure set theory to standard algebraic frameworks was a sign of its maturity. The actual merger of soft set theory and the multifaceted fuzzy model was another noteworthy

parallel comparable development. It resulted in the Complex Fuzzy Soft Set [25], a paradigm that leverages the two-dimensional information store of complex membership degrees and the parametrization of soft sets. Soon after, this hybrid was expanded to handle greater imprecision, giving rise to the Interval-Valued Complex Fuzzy Soft Set [26]. Recent advances have proposed even more powerful hybrid frameworks that can simulate complicated and higher-order uncertainty, pushing this integration to even greater heights. As an example, Fujita [27] developed strong models that can handle data represented by multi-dimensional membership degree by incorporating a hyper-fuzzy environment into the already outstanding VIKOR and DEMATEL approaches. In the same vein, Gul [28] proposed a bipolar fuzzy rough set model fused with the VIKOR approach, which offers a more detailed model on the capacity to manage conflicting criteria and is useful in reflecting the positive and negative preferences of decision-makers in a d-covering context. Alongside these advancements, the study of more complex algebraic structures has produced a solid theoretical foundation for the use of these methods in significant fields. The work of Abdalla et al. [29] on Interval-Valued Fermatean Neutrosophic Super Hyper Soft Sets is an illustration of this trend. It describes how complex forms of uncertainty in real-world contexts like health care, where the information is indeterminate, incomplete, and may come from multiple sources, can be represented by sophisticated set-theoretic models.

1.1. Literature Review

This approach was also used to combine other kinds of complex sets, resulting in Complex Vague Soft Sets [31] and Complex Intuitionistic Fuzzy Soft Sets [30], each of which has its own entropies and distance measures to make it useful. Broumi et al. made the strongest synthesis when they introduced the Complex Neutrosophic Soft Set [32], which permits the expression of truth, indeterminacy, and falsity in the complex plane while allowing the use of the parameterized method of soft sets. Scholars developed expert and prioritizing procedures in an attempt to give these models more realism in relation to actual decision-making processes. Prioritized aggregation operators of complicated intuitionistic fuzzy soft sets were constructed by Ali et al. [33], ensuring that the critical qualities are given greater weight. By splitting apart the Complex Neutrosophic Soft Expert Set, Al-Quran and Hassan directly included expert opinion into the model [34]. This line of inquiry was further expanded with the creation of the even more extensive Complex Multi-Fuzzy Soft Expert Set [35], which may address numerous membership sequences of each parameter. Last but not least, the Fuzzy Parameterized Complex Multi-Fuzzy Soft Expert Sets [36] invention added even more flexibility by allowing fuzzy sets to choose the parameters themselves. This is the extent of integrative and application-oriented evolution. The path of hybridization is always changing and expanding the possibilities for representing ambiguity and nuanced information. The recent study by AlAkram et al. [37], which suggested Complex Fermatean Fuzzy N-Soft Sets, is one example of how novel this is at the moment. This model is a significant amalgam of many potent paradigms: Last but not least, the Fuzzy Parameterized Complex Multi-Fuzzy Soft Expert Sets [36] invention added even more flexibility by allowing fuzzy sets to choose the parameters themselves. This is the extent of integrative and application-oriented evolution. The path of hybridization is always changing and expanding the possibilities for representing ambiguity and nuanced information. The recent study by AlAkram et al. [37], which suggested Complex Fermatean Fuzzy N-Soft Sets, is one example of how novel this is at the moment. This model is a significant amalgam of many potent paradigms: These three cutting-edge ideas are combined in this hybrid model to provide an unparalleled capacity for handling multi-level, complicated, and ambiguous data while making decisions. Its creation demonstrates the field's constant drive to create increasingly expressive and adaptable mathematical tools in order to represent the complexity of the real world. By establishing the Complex Bipolar-Valued Neutrosophic Soft Set [38], Al-Quran et al. advanced the research of bipolarity on the complex neutrosophic framework and improved the model's ability to handle contradictory data dimensions. Akram et al. produced Complex

Neutrosophic N-Soft Sets [39], which provide a multi-level graded structure of truth, indeterminacy, and falsity, by combining the influential idea of N-soft sets with neutrosophic theory in complex space. Formally describing the complex neutrosophic soft expert relation [40], which provides a mathematical foundation for comparing and connecting the many expert evaluations in this intricate framework, was a significant theoretical and practical leap. A theory of Interval-Valued Complex Neutrosophic Soft Sets [41] and related relations [43] also extended this relational paradigm to address imprecision. When these models were eventually articulated in complex space [42], it was a necessary generalization, and their representational power was significantly increased. Effective comparison tools are essential to all of these advancements. Similarity measurements, which are essential for applications like pattern recognition and medical diagnosis, have been the subject of extensive research as a result. Numerous structures have been developed, including Lattice Ordered Multi-Fuzzy Soft Sets [45], Single and Multi-Valued Neutrosophic Hypersoft Sets [44], and m-polar-interval valued Neutrosophic Soft Sets [46]. The real-world effects of such progressively abstract theoretical constructions are demonstrated by the practical effects of such measurements, particularly in sensitive fields like medical diagnostics [46], which completes the circle between the formulation of mathematical issues and their practical resolution. Since the proliferation of these sophisticated hybrid forms has necessitated the development of robust methods for comparing and contrasting these forms, recent studies have included research on similarity metrics and entropy. They are crucial in applications like as pattern recognition, medical diagnosis, and multi-criteria decision-making, where the ability to measure the degree of similarity or ambiguity across different sets is crucial. Basic similarity measures between neutrosophic and interval neutrosophic sets were founded by Broumi and Smarandache [50] and Ye [51], respectively. These were soon generalized to hybrid structures, as was the case with similarity measures of Interval Valued Neutrosophic Soft Sets [52]. Medical usages are also a dominant factor and Liu et al. [47] utilize the Euclidean distance to neutrosophic sets to diagnose, which Zulqarnain et al. [46] apply to more advanced m-Polar features. The comparison techniques grew more intricate as the models became more intricate. The researchers employed Lattice Ordered Multi-Fuzzy Soft Sets [45], Possibility Intuitionistic Fuzzy Hyper-soft Sets [49], and T-Spherical Fuzzy Sets [48] as special measures. The same idea holds true in the complex realm, where Complex Multi-Fuzzy Soft Sets [54] have been subjected to entropy and similarity measures in order to handle the dimensional expansion. Additionally, equivalent entropy and distance metrics have been added to generalization to structures like Q-Neutrosophic Soft Sets [53], ensuring that even the most generalized models have the mathematical resources needed to be practical. To put it simply, the creation of each new hybrid model is now entangled with the creation of the corresponding entropy and similarity metrics. This ensures that the theoretical power of such complex structures can be appropriately applied to the solution of complex real-world problems where comparison and uncertainty quantification are the best qualities. In order to address the issue of multi-criteria group decision-making, Xu et al. focused on distance measures of Interval Complex Neutrosophic Sets [56], while Selvachandran et al. developed a similarity measure on Complex Vague Soft Sets and demonstrated its applicability in pattern recognition [55]. These metrics of comparison have been developed and applied extensively on a variety of complex hybrid models. Neutrosophic set and its characteristics were studied in [57].

A fundamental idea in the field is brought to light by this consistent correlation between the new set-theoretic models and specially designed similarity and distance measures: the practice drives and validates the theory's progress. Lastly, our ability to mathematically describe uncertainty has grown exponentially since the original fuzzy sets proposed by Zadeh [1] evolved into the complex, neutrosophic, and soft hybrid models of today. This has been called a cycle of innovation, whereby a new theoretical framework is created by identifying a representational deficiency, then new components are added, and finally, real-world applications of similarity measures and aggregation operators are added to deal with the real world. The result is a

multifaceted and varied ecosystem of mathematical tools that can simulate the gradation, ambiguity, cyclicity, and intrinsic contradictions of complex systems, enabling robots to reason more like humans. Since the principles of these frameworks have been extended beyond set theory to abstract algebraic and mathematical structures, the final step of the evolutionary process demonstrates how theoretically profound they are. This development was supported by the introduction of Interval Neutrosophic Sets [59] and is based on Smarandache's early work on Neutrosophy [58], which provides the logical and philosophical underpinnings of neutrosophic logic. Fuzzy, intuitionistic, and neutrosophic notions can now be applied to basic algebraic fields thanks to this groundbreaking discovery. The operations of Intuitionistic and Interval-Valued Intuitionistic Fuzzy Soft Sets [60] have been more extensively generalized to distance measurements, which gives them an algebraic basis. Concurrently, the set-theoretic models have been expanded to include more complex models that can process multi-dimensional attribute values, as the Plithagenic Hyper-soft Set [61].

Most significantly, a robust research thread that builds algebraic systems on top of the existing uncertainty-based foundations has been produced. These include studies of structures like Intuitionistic Anti Fuzzy Normal Subrings over Normed Rings [63] and the Neutrosophic Multiplication Module [62]. The work on Polish Groups [64], conditions on P.P. Rings [65], Classical Artinian Modules [66], Fractional Ideals [67], and structures in Topological Groups [68] all point to a parallel study program in pure algebra that is extended by this subject.

This indicates that in addition to advancing these uncertainty theories, the mathematical community is also contributing to the advancement of the classical algebraic structures to which they are applied. In conclusion, it is important to note that the current state of amazing intellectual synergy is a direct result of the fuzzy sets of Zadeh. Beginning with the very simple idea of graded membership, it evolved into a whole ecosystem of models to address uncertainty through phases of integration and generalization to complex planes, neutrosophic logic, and parameterized soft sets. This evolution typically follows a positive feedback loop: theoretical innovation results in new hybrid models, which are then given useful tools like comparable measures to be applied, and their ideas are abstracted to enhance fundamental fields like abstract algebra. This leads to a dynamic and intricate area of mathematics that ultimately enhances our ability to reason, model, and navigate a world that is fundamentally complex and uncertain. The thorough examination of the structures, like the Neutrosophic Multiplication Module [62] and Intuitionistic Anti Fuzzy Normal Subrings over Normed Rings [63], continues this robust line of inquiry that seeks to create algebraic systems with uncertainty-driven foundations. As evidenced by work on Classical Artinian Modules [69], Polish Groups [64], conditions on P.P. Rings [65], Fractional Ideals [67], and the study of new types of mappings in Topological spaces with Strongly Closed Graphs [70], this line of inquiry is part of a larger, parallel research program in pure algebra and topology.

The investigation of supra open soft sets and its various decompositions and applications, as well as soft set theory, are both superseded by supra soft topology, according to the sources provided. Fundamental results on decompositions of supra soft sets, together with the concept of soft continuity in this context, were provided by El-Sheikh and Abd Ellatif's basic contributions [71]. Supra soft strongly generalized closed sets [73], supra soft strongly extra generalized closed sets [74], and supra soft strongly *semi** generalized closed sets [76] are only a few of the specific classes of soft sets that are now being studied in this field. Furthermore, the ideas have been crucial in defining and researching different forms of soft connectedness [78] as well as related soft separation axioms [72][75][77]. The research of supra soft compactness [80] and interactions with soft ideals [79] have also contributed to the development of the theory.

1.2. Novelty and Motivation for Research

This work is unique because it presents a comprehensive theoretical framework using Complex Neutrosophic Soft Sets (CNSS), which is a generalization of the current models that deals

with two-dimensional information by introducing complex-number valued membership functions. The design of a comprehensive CNSS topology, which extends set operations to the production of a formal mathematical space with concepts of interior, closure, and continuity, is one important theoretical advancement. An inventive synthesized presentation that applies the abstract paradigm to the real-world problem of signal-template alignment goes hand in hand with this conceptual innovation. The power of the framework is demonstrated by the new method, which is tested using a multifaceted visualization suite. It is able to reconcile theory and practice, revealing the specific utility of different signals and identifying the strongest pairing, $S_2 - T_1$. This research is informed by the need to explain the multifaceted, multidimensional uncertainty that contemporary data (signals and time series) must convey. This uncertainty includes both statistical randomness and cognitive imprecision, such as vagueness.

Current fuzzy and neutrosophic models, which are primarily designed to handle real-valued input, do not achieve the two-fold complexity. Furthermore, there is a significant gap between higher mathematical theory and real data analysis, necessitating the use of more thorough and instructive analytical tools that can serve as a strong foundation for the belief in sophisticated data reasoning.

2. Preliminaries

We offer some basic terminology and background information in this part that will be helpful as our investigation develops further.

Definition 1. [57] *The expression for a neutrosophic set A defined on a discourse universe \mathbb{X} is*

$$A = \{ \langle x, T_A(x), I_A(x), F_A(x) \rangle : x \in \mathbb{X} \}$$

where, $T, I, F : \mathbb{X} \rightarrow]0, 1[$ and $0 \leq T_A(x) + I_A(x) + F_A(x) \leq 3$.

Definition 2. [14] *Let $P(\mathbb{X})$ be the power set of \mathbb{X} , \mathbb{X} be a universal set, and $\acute{\mathcal{E}}$ be a collection of parameters. When \mathcal{F} is a mapping $\mathcal{F} : \acute{\mathcal{E}} \rightarrow P(\mathbb{X})$, then $(\mathcal{F}, \acute{\mathcal{E}})$ is referred to as a soft set over \mathbb{X} . Put differently, a parameterized family of subsets of \mathbb{X} is referred to as a soft set. The set of \mathfrak{e} -elements of the soft set $(\mathcal{F}, \acute{\mathcal{E}})$, or the set of \mathfrak{e} -approximate elements of the soft set, is represented by $\mathcal{F}(\mathfrak{e})$ for each parameter $\mathfrak{e} \in \acute{\mathcal{E}}$, i.e.,*

$$(\mathcal{F}, \acute{\mathcal{E}}) = \{ (\mathfrak{e}, \mathcal{F}(\mathfrak{e})) : \mathfrak{e} \in \acute{\mathcal{E}}, \mathcal{F} : \acute{\mathcal{E}} \rightarrow P(\mathbb{X}) \}$$

Maji [19] was the first to propose the idea of the neutrosophic soft set, which Deli and Broumi [20] later developed as described below.

Definition 3. *Let $\acute{\mathcal{E}}$ be a set of parameters and \mathbb{X} be a universal set. The collection of all neutrosophic sets on \mathbb{X} is represented by $P(\mathbb{X})$. An approximate function of the neutrosophic soft set $(\tilde{\mathcal{F}}, \acute{\mathcal{E}})$ is $\tilde{\mathcal{F}}$, where $\tilde{\mathcal{F}}$ is defined by a set valued function $\tilde{\mathcal{F}} : \acute{\mathcal{E}} \rightarrow P(\mathbb{X})$. It can be expressed as a parameterized family of neutrosophic sets on $P(\mathbb{X})$.*

$$(\tilde{\mathcal{F}}, \acute{\mathcal{E}}) = \{ (\mathfrak{e}, \langle x, T_{\tilde{\mathcal{F}}(\mathfrak{e})}(x), I_{\tilde{\mathcal{F}}(\mathfrak{e})}(x), F_{\tilde{\mathcal{F}}(\mathfrak{e})}(x) \rangle : x \in \mathbb{X} : \mathfrak{e} \in \acute{\mathcal{E}} \}$$

where $T_{\tilde{\mathcal{F}}(\mathfrak{e})}(x), I_{\tilde{\mathcal{F}}(\mathfrak{e})}(x), F_{\tilde{\mathcal{F}}(\mathfrak{e})}(x) \in [0, 1]$ are the truth membership, indeterminacy membership, and falsity membership of $\tilde{\mathcal{F}}(\mathfrak{e})$. The inequality $0 \leq T_{\tilde{\mathcal{F}}(\mathfrak{e})}(x) + I_{\tilde{\mathcal{F}}(\mathfrak{e})}(x) + F_{\tilde{\mathcal{F}}(\mathfrak{e})}(x) \leq 3$ is evident since the supremum of each $T, I, \text{and } F$ is 1.

Definition 4. [21] *Consider the neutrosophic soft set $(\tilde{\mathcal{F}}, \acute{\mathcal{E}})$ on \mathbb{X} . $(\tilde{\mathcal{F}}, \acute{\mathcal{E}})^c$ represents the complement of $(\tilde{\mathcal{F}}, \acute{\mathcal{E}})$, which is defined by:*

$$(\tilde{\mathcal{F}}, \acute{\mathcal{E}})^c = \{ (\mathfrak{e}, \langle x, F_{\tilde{\mathcal{F}}(\mathfrak{e})}(x), 1 - I_{\tilde{\mathcal{F}}(\mathfrak{e})}(x), T_{\tilde{\mathcal{F}}(\mathfrak{e})}(x) \rangle : x \in \mathbb{X} : \mathfrak{e} \in \acute{\mathcal{E}} \}$$

$((\tilde{\mathcal{F}}, \acute{\mathcal{E}})^c)^c = (\tilde{\mathcal{F}}, \acute{\mathcal{E}})$ is clearly true.

Definition 5. [19] Assume that $(\tilde{\mathcal{F}}, \mathcal{E})$ and $(\tilde{\mathcal{G}}, \mathcal{E})$ are neutrosophic soft sets on \mathbb{X} . $(\tilde{\mathcal{F}}, \mathcal{E})$ is the neutrosophic soft subset of $(\tilde{\mathcal{G}}, \mathcal{E})$ if $T_{\tilde{\mathcal{F}}(\mathfrak{e})}(x) \leq T_{\tilde{\mathcal{G}}(\mathfrak{e})}(x), I_{\tilde{\mathcal{F}}(\mathfrak{e})}(x) \leq I_{\tilde{\mathcal{G}}(\mathfrak{e})}(x), F_{\tilde{\mathcal{F}}(\mathfrak{e})}(x) \geq F_{\tilde{\mathcal{G}}(\mathfrak{e})}(x)$, for every $x \in \mathbb{X}$, for every $\mathfrak{e} \in \mathcal{E}$. $(\tilde{\mathcal{F}}, \mathcal{E}) \subseteq (\tilde{\mathcal{G}}, \mathcal{E})$ is the notation for it. $(\tilde{\mathcal{F}}, \mathcal{E})$ is neutrosophic soft set equal to $(\tilde{\mathcal{G}}, \mathcal{E})$ if $(\tilde{\mathcal{F}}, \mathcal{E})$ is a neutrosophic soft subset of $(\tilde{\mathcal{G}}, \mathcal{E})$ and $(\tilde{\mathcal{G}}, \mathcal{E})$ is a soft neutrosophic subset of $(\tilde{\mathcal{F}}, \mathcal{E})$. $(\tilde{\mathcal{F}}, \mathcal{E}) = (\tilde{\mathcal{G}}, \mathcal{E})$ is the notation for it.

3. Fundamentals of Complex Neutrosophic Soft Sets

This section is devoted to the basic operations which are helpful for the upcoming sections.

Definition 6. Consider the CNS sets $(\tilde{\mathcal{F}}_1, \mathcal{E})$ and $(\tilde{\mathcal{F}}_2, \mathcal{E})$ on \mathbb{X} then their union is represented as $(\tilde{\mathcal{F}}_1, \mathcal{E}) \uplus (\tilde{\mathcal{F}}_2, \mathcal{E}) = (\tilde{\mathcal{F}}_3, \mathcal{E})$ is signified by:

$$(\tilde{\mathcal{F}}_3, \mathcal{E}) = \left\{ \left(\mathfrak{e}, \langle x, T_{\tilde{\mathcal{F}}_3(\mathfrak{e})}(x), I_{\tilde{\mathcal{F}}_3(\mathfrak{e})}(x), F_{\tilde{\mathcal{F}}_3(\mathfrak{e})}(x) \rangle : x \in \mathbb{X} \right) : \mathfrak{e} \in \mathcal{E} \right\},$$

where

$$\begin{aligned} T_{\tilde{\mathcal{F}}_3(\mathfrak{e})}(x) &= \max\{T_{\tilde{\mathcal{F}}_1(\mathfrak{e})}(x), T_{\tilde{\mathcal{F}}_2(\mathfrak{e})}(x)\} \\ I_{\tilde{\mathcal{F}}_3(\mathfrak{e})}(x) &= \max\{I_{\tilde{\mathcal{F}}_1(\mathfrak{e})}(x), I_{\tilde{\mathcal{F}}_2(\mathfrak{e})}(x)\} \\ F_{\tilde{\mathcal{F}}_3(\mathfrak{e})}(x) &= \min\{F_{\tilde{\mathcal{F}}_1(\mathfrak{e})}(x), F_{\tilde{\mathcal{F}}_2(\mathfrak{e})}(x)\} \end{aligned}$$

Definition 7. Consider the CNS sets $(\tilde{\mathcal{F}}_1, \mathcal{E})$ and $(\tilde{\mathcal{F}}_2, \mathcal{E})$ on \mathbb{X} . The expression for their intersection is $(\tilde{\mathcal{F}}_1, \mathcal{E}) \cap (\tilde{\mathcal{F}}_2, \mathcal{E}) = (\tilde{\mathcal{F}}_3, \mathcal{E})$. defined as:

$$(\tilde{\mathcal{F}}_3, \mathcal{E}) = \left\{ \left(\mathfrak{e}, \langle x, T_{\tilde{\mathcal{F}}_3(\mathfrak{e})}(x), I_{\tilde{\mathcal{F}}_3(\mathfrak{e})}(x), F_{\tilde{\mathcal{F}}_3(\mathfrak{e})}(x) \rangle : x \in \mathbb{X} \right) : \mathfrak{e} \in \mathcal{E} \right\},$$

Where

$$\begin{aligned} T_{\tilde{\mathcal{F}}_3(\mathfrak{e})}(x) &= \min\{T_{\tilde{\mathcal{F}}_1(\mathfrak{e})}(x), T_{\tilde{\mathcal{F}}_2(\mathfrak{e})}(x)\} \\ I_{\tilde{\mathcal{F}}_3(\mathfrak{e})}(x) &= \min\{I_{\tilde{\mathcal{F}}_1(\mathfrak{e})}(x), I_{\tilde{\mathcal{F}}_2(\mathfrak{e})}(x)\} \\ F_{\tilde{\mathcal{F}}_3(\mathfrak{e})}(x) &= \max\{F_{\tilde{\mathcal{F}}_1(\mathfrak{e})}(x), F_{\tilde{\mathcal{F}}_2(\mathfrak{e})}(x)\} \end{aligned}$$

Definition 8. Consider the CNS sets $(\tilde{\mathcal{F}}_1, \mathcal{E})$ and $(\tilde{\mathcal{F}}_2, \mathcal{E})$ on \mathbb{X} . Then, $(\tilde{\mathcal{F}}_1, \mathcal{E})$ difference $(\tilde{\mathcal{F}}_2, \mathcal{E})$ operation on these sets is represented by $(\tilde{\mathcal{F}}_1, \mathcal{E}) \setminus (\tilde{\mathcal{F}}_2, \mathcal{E}) = (\tilde{\mathcal{F}}_3, \mathcal{E})$, and is given as $(\tilde{\mathcal{F}}_1, \mathcal{E}) \cap (\tilde{\mathcal{F}}_2, \mathcal{E})^c = (\tilde{\mathcal{F}}_3, \mathcal{E})$

$$(\tilde{\mathcal{F}}_3, \mathcal{E}) = \left\{ \left(\mathfrak{e}, \langle x, T_{\tilde{\mathcal{F}}_3(\mathfrak{e})}(x), I_{\tilde{\mathcal{F}}_3(\mathfrak{e})}(x), F_{\tilde{\mathcal{F}}_3(\mathfrak{e})}(x) \rangle : x \in \mathbb{X} \right) : \mathfrak{e} \in \mathcal{E} \right\},$$

where

$$\begin{aligned} T_{\tilde{\mathcal{F}}_3(\mathfrak{e})}(x) &= \min\{T_{\tilde{\mathcal{F}}_1(\mathfrak{e})}(x), F_{\tilde{\mathcal{F}}_2(\mathfrak{e})}(x)\} \\ I_{\tilde{\mathcal{F}}_3(\mathfrak{e})}(x) &= \min\{I_{\tilde{\mathcal{F}}_1(\mathfrak{e})}(x), 1 - I_{\tilde{\mathcal{F}}_2(\mathfrak{e})}(x)\} \\ F_{\tilde{\mathcal{F}}_3(\mathfrak{e})}(x) &= \max\{F_{\tilde{\mathcal{F}}_1(\mathfrak{e})}(x), T_{\tilde{\mathcal{F}}_2(\mathfrak{e})}(x)\} \end{aligned}$$

Definition 9. Suppose that $\{(\tilde{\mathcal{F}}_i, \mathcal{E}) : i \in I\}$ be a collection of CNS sets defined on \mathbb{X} . So,

$$\begin{aligned} \bigcup_{i \in I} (\tilde{\mathcal{F}}_i, \mathcal{E}) &= \left\{ \left(\mathfrak{e}, \langle x, \sup_{i \in I} T_{\tilde{\mathcal{F}}_i(\mathfrak{e})}(x), \sup_{i \in I} I_{\tilde{\mathcal{F}}_i(\mathfrak{e})}(x), \inf_{i \in I} F_{\tilde{\mathcal{F}}_i(\mathfrak{e})}(x) \rangle : x \in \mathbb{X} \right) : \mathfrak{e} \in \mathcal{E} \right\}. \\ \bigcap_{i \in I} (\tilde{\mathcal{F}}_i, \mathcal{E}) &= \left\{ \left(\mathfrak{e}, \langle x, \inf_{i \in I} T_{\tilde{\mathcal{F}}_i(\mathfrak{e})}(x), \inf_{i \in I} I_{\tilde{\mathcal{F}}_i(\mathfrak{e})}(x), \sup_{i \in I} F_{\tilde{\mathcal{F}}_i(\mathfrak{e})}(x) \rangle : x \in \mathbb{X} \right) : \mathfrak{e} \in \mathcal{E} \right\}. \end{aligned}$$

Definition 10. Consider the CNS sets $(\tilde{\mathcal{F}}_1, \mathcal{E})$ and $(\tilde{\mathcal{F}}_2, \mathcal{E})$ on \mathbb{X} . The AND operation between them is then expressed as: $(\tilde{\mathcal{F}}_1, \mathcal{E}) \wedge (\tilde{\mathcal{F}}_2, \mathcal{E}) = (\tilde{\mathcal{F}}_3, \mathcal{E} \times \mathcal{E})$

$$(\tilde{\mathcal{F}}, \mathcal{E} \times \mathcal{E}) = \left\{ \left((\mathfrak{e}_1, \mathfrak{e}_2), \langle x, T_{\tilde{\mathcal{F}}_3(\mathfrak{e}_1, \mathfrak{e}_2)}(x), I_{\tilde{\mathcal{F}}_3(\mathfrak{e}_1, \mathfrak{e}_2)}(x), F_{\tilde{\mathcal{F}}_3(\mathfrak{e}_1, \mathfrak{e}_2)}(x) \rangle : x \in \mathbb{X} \right) : (\mathfrak{e}_1, \mathfrak{e}_2) \in \mathcal{E} \times \mathcal{E} \right\}.$$

where

$$\begin{aligned} T_{\tilde{\mathcal{F}}_3(\mathfrak{e}_1, \mathfrak{e}_2)}(x) &= \min \left\{ T_{\tilde{\mathcal{F}}_1(\mathfrak{e}_1, \mathfrak{e}_2)}(x), T_{\tilde{\mathcal{F}}_2(\mathfrak{e}_1, \mathfrak{e}_2)}(x) \right\}, \\ I_{\tilde{\mathcal{F}}_3(\mathfrak{e}_1, \mathfrak{e}_2)}(x) &= \min \left\{ I_{\tilde{\mathcal{F}}_1(\mathfrak{e}_1, \mathfrak{e}_2)}(x), I_{\tilde{\mathcal{F}}_2(\mathfrak{e}_1, \mathfrak{e}_2)}(x) \right\}, \\ F_{\tilde{\mathcal{F}}_3(\mathfrak{e}_1, \mathfrak{e}_2)}(x) &= \max \left\{ F_{\tilde{\mathcal{F}}_1(\mathfrak{e}_1, \mathfrak{e}_2)}(x), F_{\tilde{\mathcal{F}}_2(\mathfrak{e}_1, \mathfrak{e}_2)}(x) \right\}. \end{aligned}$$

Definition 11. Consider the CNS sets $(\tilde{\mathcal{F}}_1, \mathcal{E})$ and $(\tilde{\mathcal{F}}_2, \mathcal{E})$ on \mathbb{X} . The OR operation that is then applied to these sets is indicated by $(\tilde{\mathcal{F}}_1, \mathcal{E}) \vee (\tilde{\mathcal{F}}_2, \mathcal{E}) = (\tilde{\mathcal{F}}_3, \mathcal{E} \times \mathcal{E})$ and is given by:

$$(\tilde{\mathcal{F}}, \mathcal{E} \times \mathcal{E}) = \left\{ \left((\mathfrak{e}_1, \mathfrak{e}_2), \langle x, T_{\tilde{\mathcal{F}}_3(\mathfrak{e}_1, \mathfrak{e}_2)}(x), I_{\tilde{\mathcal{F}}_3(\mathfrak{e}_1, \mathfrak{e}_2)}(x), F_{\tilde{\mathcal{F}}_3(\mathfrak{e}_1, \mathfrak{e}_2)}(x) \rangle : x \in \mathbb{X} \right) : (\mathfrak{e}_1, \mathfrak{e}_2) \in \mathcal{E} \times \mathcal{E} \right\}.$$

where

$$\begin{aligned} T_{\tilde{\mathcal{F}}_3(\mathfrak{e}_1, \mathfrak{e}_2)}(x) &= \max \left\{ T_{\tilde{\mathcal{F}}_1(\mathfrak{e}_1, \mathfrak{e}_2)}(x), T_{\tilde{\mathcal{F}}_2(\mathfrak{e}_1, \mathfrak{e}_2)}(x) \right\}, \\ I_{\tilde{\mathcal{F}}_3(\mathfrak{e}_1, \mathfrak{e}_2)}(x) &= \max \left\{ I_{\tilde{\mathcal{F}}_1(\mathfrak{e}_1, \mathfrak{e}_2)}(x), I_{\tilde{\mathcal{F}}_2(\mathfrak{e}_1, \mathfrak{e}_2)}(x) \right\}, \\ F_{\tilde{\mathcal{F}}_3(\mathfrak{e}_1, \mathfrak{e}_2)}(x) &= \min \left\{ F_{\tilde{\mathcal{F}}_1(\mathfrak{e}_1, \mathfrak{e}_2)}(x), F_{\tilde{\mathcal{F}}_2(\mathfrak{e}_1, \mathfrak{e}_2)}(x) \right\}. \end{aligned}$$

Definition 12. A null CNS set is defined as a CNS set $(\tilde{\mathcal{F}}, \mathcal{E})$ on \mathbb{X} if

$$T_{\tilde{\mathcal{F}}(\mathfrak{e})}(x) = 0, \quad I_{\tilde{\mathcal{F}}(\mathfrak{e})}(x) = 0, \quad F_{\tilde{\mathcal{F}}(\mathfrak{e})}(x) = 1, \quad \forall \mathfrak{e} \in \mathcal{E}, \forall x \in \mathbb{X}.$$

$0_{(\mathbb{X}, \mathcal{E})}$ is the symbol for it.

Definition 13. $(\tilde{\mathcal{F}}, \mathcal{E})$ on \mathbb{X} is referred to as a CNS set absolute CNS set if

$$T_{\tilde{\mathcal{F}}(\mathfrak{e})}(x) = 1, \quad I_{\tilde{\mathcal{F}}(\mathfrak{e})}(x) = 1, \quad F_{\tilde{\mathcal{F}}(\mathfrak{e})}(x) = 0, \quad \forall \mathfrak{e} \in \mathcal{E}, \forall x \in \mathbb{X},$$

Evidently,

$$0_{(\mathbb{X}, \mathcal{E})}^c = 1_{(\mathbb{X}, \mathcal{E})}, \quad 1_{(\mathbb{X}, \mathcal{E})}^c = 0_{(\mathbb{X}, \mathcal{E})}.$$

Proposition 1. Assume that $(\tilde{\mathcal{F}}_1, \mathcal{E})$ and $(\tilde{\mathcal{F}}_2, \mathcal{E})$ as well as $(\tilde{\mathcal{F}}_3, \mathcal{E})$ are CNS sets on \mathbb{X} . Then,

- (i) $(\tilde{\mathcal{F}}_1, \mathcal{E}) \cup [(\tilde{\mathcal{F}}_2, \mathcal{E}) \cup (\tilde{\mathcal{F}}_3, \mathcal{E})] = [(\tilde{\mathcal{F}}_1, \mathcal{E}) \cup (\tilde{\mathcal{F}}_2, \mathcal{E})] \cup (\tilde{\mathcal{F}}_3, \mathcal{E})$ and $(\tilde{\mathcal{F}}_1, \mathcal{E}) \cap [(\tilde{\mathcal{F}}_2, \mathcal{E}) \cap (\tilde{\mathcal{F}}_3, \mathcal{E})] = [(\tilde{\mathcal{F}}_1, \mathcal{E}) \cap (\tilde{\mathcal{F}}_2, \mathcal{E})] \cap (\tilde{\mathcal{F}}_3, \mathcal{E})$;
- (ii) $(\tilde{\mathcal{F}}_1, \mathcal{E}) \cup [(\tilde{\mathcal{F}}_2, \mathcal{E}) \cap (\tilde{\mathcal{F}}_3, \mathcal{E})] = [(\tilde{\mathcal{F}}_1, \mathcal{E}) \cup (\tilde{\mathcal{F}}_2, \mathcal{E})] \cap [(\tilde{\mathcal{F}}_1, \mathcal{E}) \cup (\tilde{\mathcal{F}}_3, \mathcal{E})]$ and $(\tilde{\mathcal{F}}_1, \mathcal{E}) \cap [(\tilde{\mathcal{F}}_2, \mathcal{E}) \cup (\tilde{\mathcal{F}}_3, \mathcal{E})] = [(\tilde{\mathcal{F}}_1, \mathcal{E}) \cap (\tilde{\mathcal{F}}_2, \mathcal{E})] \cup [(\tilde{\mathcal{F}}_1, \mathcal{E}) \cap (\tilde{\mathcal{F}}_3, \mathcal{E})]$;
- (iii) $(\tilde{\mathcal{F}}_1, \mathcal{E}) \cup 0_{(\mathbb{X}, \mathcal{E})} = (\tilde{\mathcal{F}}_1, \mathcal{E})$ and $(\tilde{\mathcal{F}}_1, \mathcal{E}) \cap 0_{(\mathbb{X}, \mathcal{E})} = 0_{(\mathbb{X}, \mathcal{E})}$;
- (iv) $(\tilde{\mathcal{F}}_1, \mathcal{E}) \cup 1_{(\mathbb{X}, \mathcal{E})} = (\tilde{\mathcal{F}}_1, \mathcal{E})$ and $(\tilde{\mathcal{F}}_1, \mathcal{E}) \cap 1_{(\mathbb{X}, \mathcal{E})} = (\tilde{\mathcal{F}}_1, \mathcal{E})$;

Proof. Obvious.

Proposition 2. Suppose that $(\tilde{\mathcal{F}}_1, \mathcal{E})$ and $(\tilde{\mathcal{F}}_2, \mathcal{E})$ be CNS sets on \mathbb{X} which exist. Then,

$$(i) [(\tilde{\mathcal{F}}_1, \mathcal{E}) \cup (\tilde{\mathcal{F}}_2, \mathcal{E})]^c = (\tilde{\mathcal{F}}_1, \mathcal{E})^c \cap (\tilde{\mathcal{F}}_2, \mathcal{E})^c$$

$$(ii) [(\tilde{\mathcal{F}}_1, \mathcal{E}) \cap (\tilde{\mathcal{F}}_2, \mathcal{E})]^c = (\tilde{\mathcal{F}}_1, \mathcal{E})^c \cup (\tilde{\mathcal{F}}_2, \mathcal{E})^c$$

Proof. (i). $\forall x \in \mathbb{X}$ and $e \in \mathcal{E}$,

$$\begin{aligned} (\tilde{\mathcal{F}}_1, \mathcal{E}) \cup (\tilde{\mathcal{F}}_2, \mathcal{E}) &= \{ \langle x, \max\{T_{\tilde{\mathcal{F}}_1(e)}(x), T_{\tilde{\mathcal{F}}_2(e)}(x)\}, \max\{I_{\tilde{\mathcal{F}}_1(e)}(x), I_{\tilde{\mathcal{F}}_2(e)}(x)\}, \\ &\quad \min\{F_{\tilde{\mathcal{F}}_1(e)}(x), F_{\tilde{\mathcal{F}}_2(e)}(x)\} \rangle \} \\ [(\tilde{\mathcal{F}}_1, \mathcal{E}) \cup (\tilde{\mathcal{F}}_2, \mathcal{E})]^c &= \{ \langle x, \min\{F_{\tilde{\mathcal{F}}_1(e)}(x), F_{\tilde{\mathcal{F}}_2(e)}(x)\}, 1 - \max\{I_{\tilde{\mathcal{F}}_1(e)}(x), I_{\tilde{\mathcal{F}}_2(e)}(x)\}, \\ &\quad \max\{T_{\tilde{\mathcal{F}}_1(e)}(x), T_{\tilde{\mathcal{F}}_2(e)}(x)\} \rangle \} \end{aligned}$$

Now,

$$\begin{aligned} (\tilde{\mathcal{F}}_1, \mathcal{E})^c &= \{ \langle x, F_{\tilde{\mathcal{F}}_1(e)}(x), 1 - I_{\tilde{\mathcal{F}}_1(e)}(x), T_{\tilde{\mathcal{F}}_1(e)}(x) \rangle \} \\ (\tilde{\mathcal{F}}_2, \mathcal{E})^c &= \{ \langle x, F_{\tilde{\mathcal{F}}_2(e)}(x), 1 - I_{\tilde{\mathcal{F}}_2(e)}(x), T_{\tilde{\mathcal{F}}_2(e)}(x) \rangle \} \end{aligned}$$

So,

$$\begin{aligned} (\tilde{\mathcal{F}}_1, \mathcal{E})^c \cap (\tilde{\mathcal{F}}_2, \mathcal{E})^c &= \{ \langle x, \min\{F_{\tilde{\mathcal{F}}_1(e)}(x), F_{\tilde{\mathcal{F}}_2(e)}(x)\}, \min\{1 - I_{\tilde{\mathcal{F}}_1(e)}(x), 1 - I_{\tilde{\mathcal{F}}_2(e)}(x)\}, \\ &\quad \max\{T_{\tilde{\mathcal{F}}_1(e)}(x), T_{\tilde{\mathcal{F}}_2(e)}(x)\} \rangle \} \\ &= \{ \langle x, \min\{F_{\tilde{\mathcal{F}}_1(e)}(x), F_{\tilde{\mathcal{F}}_2(e)}(x)\}, 1 - \max\{I_{\tilde{\mathcal{F}}_1(e)}(x), I_{\tilde{\mathcal{F}}_2(e)}(x)\}, \\ &\quad \max\{T_{\tilde{\mathcal{F}}_1(e)}(x), T_{\tilde{\mathcal{F}}_2(e)}(x)\} \rangle \} \end{aligned}$$

Hence, $[(\tilde{\mathcal{F}}_1, \mathcal{E}) \cup (\tilde{\mathcal{F}}_2, \mathcal{E})]^c = (\tilde{\mathcal{F}}_1, \mathcal{E})^c \cap (\tilde{\mathcal{F}}_2, \mathcal{E})^c$.

(ii). It can be derived in an analogous manner.

Proposition 3. Suppose that $(\tilde{\mathcal{F}}_1, \mathcal{E})$ and $(\tilde{\mathcal{F}}_2, \mathcal{E})$ be CNS sets on \mathbb{X} which exist. Then,

$$(i) [(\tilde{\mathcal{F}}_1, \mathcal{E}) \vee (\tilde{\mathcal{F}}_2, \mathcal{E})]^c = (\tilde{\mathcal{F}}_1, \mathcal{E})^c \wedge (\tilde{\mathcal{F}}_2, \mathcal{E})^c$$

$$(ii) [(\tilde{\mathcal{F}}_1, \mathcal{E}) \wedge (\tilde{\mathcal{F}}_2, \mathcal{E})]^c = (\tilde{\mathcal{F}}_1, \mathcal{E})^c \vee (\tilde{\mathcal{F}}_2, \mathcal{E})^c$$

Proof. (i). $\forall e \in \mathcal{E}$ and $x \in \mathbb{X}$,

$$\begin{aligned} (\tilde{\mathcal{F}}_1, \mathcal{E}) \vee (\tilde{\mathcal{F}}_2, \mathcal{E}) &= \{ \langle x, \max\{T_{\tilde{\mathcal{F}}_1(e)}(x), T_{\tilde{\mathcal{F}}_2(e)}(x)\}, \max\{I_{\tilde{\mathcal{F}}_1(e)}(x), I_{\tilde{\mathcal{F}}_2(e)}(x)\}, \\ &\quad \min\{F_{\tilde{\mathcal{F}}_1(e)}(x), F_{\tilde{\mathcal{F}}_2(e)}(x)\} \rangle \} \\ [(\tilde{\mathcal{F}}_1, \mathcal{E}) \vee (\tilde{\mathcal{F}}_2, \mathcal{E})]^c &= \{ \langle x, \min\{F_{\tilde{\mathcal{F}}_1(e)}(x), F_{\tilde{\mathcal{F}}_2(e)}(x)\}, 1 - \max\{I_{\tilde{\mathcal{F}}_1(e)}(x), I_{\tilde{\mathcal{F}}_2(e)}(x)\}, \\ &\quad \max\{T_{\tilde{\mathcal{F}}_1(e)}(x), T_{\tilde{\mathcal{F}}_2(e)}(x)\} \rangle \}, \end{aligned}$$

On the other hand,

$$\begin{aligned} (\tilde{\mathcal{F}}_1, \mathcal{E})^c &= \{ \langle x, F_{\tilde{\mathcal{F}}_1(e)}(x), 1 - I_{\tilde{\mathcal{F}}_1(e)}(x), T_{\tilde{\mathcal{F}}_1(e)}(x) \rangle \} \\ (\tilde{\mathcal{F}}_2, \mathcal{E})^c &= \{ \langle x, F_{\tilde{\mathcal{F}}_2(e)}(x), 1 - I_{\tilde{\mathcal{F}}_2(e)}(x), T_{\tilde{\mathcal{F}}_2(e)}(x) \rangle \} \end{aligned}$$

So,

$$(\tilde{\mathcal{F}}_1, \mathcal{E})^c \wedge (\tilde{\mathcal{F}}_2, \mathcal{E})^c = \{ \langle x, \min\{F_{\tilde{\mathcal{F}}_1(e)}(x), F_{\tilde{\mathcal{F}}_2(e)}(x)\}, \min\{1 - I_{\tilde{\mathcal{F}}_1(e)}(x), 1 - I_{\tilde{\mathcal{F}}_2(e)}(x)\} \rangle \}$$

$$\begin{aligned} & \max\{T_{\tilde{\mathcal{F}}_1(\mathfrak{e})}(x), T_{\tilde{\mathcal{F}}_2(\mathfrak{e})}(x)\} \\ &= \{x, \min\{F_{\tilde{\mathcal{F}}_1(\mathfrak{e})}(x), F_{\tilde{\mathcal{F}}_2(\mathfrak{e})}(x)\}, 1 - \max\{I_{\tilde{\mathcal{F}}_1(\mathfrak{e})}(x), I_{\tilde{\mathcal{F}}_2(\mathfrak{e})}(x)\}, \\ & \max\{T_{\tilde{\mathcal{F}}_1(\mathfrak{e})}(x), T_{\tilde{\mathcal{F}}_2(\mathfrak{e})}(x)\}\}, \end{aligned}$$

Hence, $[(\tilde{\mathcal{F}}_1, \tilde{\mathcal{E}}) \vee (\tilde{\mathcal{F}}_2, \tilde{\mathcal{E}})]^c = (\tilde{\mathcal{F}}_1, \tilde{\mathcal{E}})^c \wedge (\tilde{\mathcal{F}}_2, \tilde{\mathcal{E}})^c$.
(ii). It is obvious.

Example 1. Let \mathbb{X} denote the universe set, defined as $\mathbb{X} = \{x_1, x_2, x_3, x_4\}$ and the parameter set is $\mathcal{E} = (\mathfrak{e}_1, \mathfrak{e}_2)$. Consider the CNS sets $(\tilde{\mathcal{F}}_1, \tilde{\mathcal{E}})$ and $(\tilde{\mathcal{F}}_2, \tilde{\mathcal{E}})$ on \mathbb{X} defined as follows;

$$(\tilde{\mathcal{F}}_1, \tilde{\mathcal{E}}) = \begin{bmatrix} \mathfrak{e}_1 = \langle x_1, 0.3e^{\iota\pi(0.2)}, 0.4e^{\iota\pi(0.3)}, 0.6e^{\iota\pi(0.5)} \rangle, \langle x_2, 0.4e^{\iota\pi(0.3)}, 0.2e^{\iota\pi(0.1)}, 0.8e^{\iota\pi(0.7)} \rangle, \\ \langle x_3, 0.6e^{\iota\pi(0.5)}, 0.2e^{\iota\pi(0.1)}, 0.5e^{\iota\pi(0.4)} \rangle, \langle x_4, 0.2e^{\iota\pi(0.1)}, 0.3e^{\iota\pi(0.2)}, 0.4e^{\iota\pi(0.3)} \rangle \\ \mathfrak{e}_2 = \langle x_1, 0.4e^{\iota\pi(0.3)}, 0.3e^{\iota\pi(0.2)}, 0.8e^{\iota\pi(0.7)} \rangle, \langle x_2, 0.3e^{\iota\pi(0.2)}, 0.4e^{\iota\pi(0.3)}, 0.2e^{\iota\pi(0.1)} \rangle, \\ \langle x_3, 0.3e^{\iota\pi(0.2)}, 0.2e^{\iota\pi(0.1)}, 0.7e^{\iota\pi(0.6)} \rangle, \langle x_4, 0.1e^{\iota\pi(0.1)}, 0.2e^{\iota\pi(0.1)}, 0.9e^{\iota\pi(0.8)} \rangle \end{bmatrix}$$

$$(\tilde{\mathcal{F}}_2, \tilde{\mathcal{E}}) = \begin{bmatrix} \mathfrak{e}_1 = \langle x_1, 0.6e^{\iota\pi(0.5)}, 0.3e^{\iota\pi(0.2)}, 0.8e^{\iota\pi(0.7)} \rangle, \langle x_2, 0.2e^{\iota\pi(0.1)}, 0.5e^{\iota\pi(0.4)}, 0.8e^{\iota\pi(0.7)} \rangle, \\ \langle x_3, 0.1e^{\iota\pi(0.1)}, 0.1e^{\iota\pi(0.1)}, 0.4e^{\iota\pi(0.3)} \rangle, \langle x_4, 0.5e^{\iota\pi(0.4)}, 0.2e^{\iota\pi(0.1)}, 0.3e^{\iota\pi(0.2)} \rangle \\ \mathfrak{e}_2 = \langle x_1, 0.7e^{\iota\pi(0.6)}, 0.5e^{\iota\pi(0.4)}, 0.6e^{\iota\pi(0.5)} \rangle, \langle x_2, 0.4e^{\iota\pi(0.3)}, 0.2e^{\iota\pi(0.1)}, 0.3e^{\iota\pi(0.2)} \rangle, \\ \langle x_3, 0.5e^{\iota\pi(0.4)}, 0.3e^{\iota\pi(0.2)}, 0.4e^{\iota\pi(0.3)} \rangle, \langle x_4, 0.4e^{\iota\pi(0.3)}, 0.2e^{\iota\pi(0.1)}, 0.6e^{\iota\pi(0.5)} \rangle \end{bmatrix}$$

The union, intersection, AND, and OR operations for these sets are expressed as follows:

$$(\tilde{\mathcal{F}}_1, \tilde{\mathcal{E}}) \cup (\tilde{\mathcal{F}}_2, \tilde{\mathcal{E}}) = \begin{bmatrix} \mathfrak{e}_1 = \langle x_1, 0.6e^{\iota\pi(0.5)}, 0.4e^{\iota\pi(0.3)}, 0.6e^{\iota\pi(0.5)} \rangle, \langle x_2, 0.4e^{\iota\pi(0.3)}, 0.5e^{\iota\pi(0.4)}, 0.8e^{\iota\pi(0.7)} \rangle, \\ \langle x_3, 0.6e^{\iota\pi(0.5)}, 0.2e^{\iota\pi(0.1)}, 0.4e^{\iota\pi(0.3)} \rangle, \langle x_4, 0.5e^{\iota\pi(0.4)}, 0.3e^{\iota\pi(0.2)}, 0.3e^{\iota\pi(0.2)} \rangle \\ \mathfrak{e}_2 = \langle x_1, 0.7e^{\iota\pi(0.6)}, 0.5e^{\iota\pi(0.4)}, 0.6e^{\iota\pi(0.5)} \rangle, \langle x_2, 0.4e^{\iota\pi(0.3)}, 0.4e^{\iota\pi(0.3)}, 0.2e^{\iota\pi(0.1)} \rangle, \\ \langle x_3, 0.5e^{\iota\pi(0.4)}, 0.3e^{\iota\pi(0.2)}, 0.4e^{\iota\pi(0.3)} \rangle, \langle x_4, 0.4e^{\iota\pi(0.3)}, 0.2e^{\iota\pi(0.1)}, 0.6e^{\iota\pi(0.5)} \rangle \end{bmatrix}$$

$$(\tilde{\mathcal{F}}_1, \tilde{\mathcal{E}}) \cap (\tilde{\mathcal{F}}_2, \tilde{\mathcal{E}}) = \begin{bmatrix} \mathfrak{e}_1 = \langle x_1, 0.3e^{\iota\pi(0.2)}, 0.3e^{\iota\pi(0.3)}, 0.8e^{\iota\pi(0.7)} \rangle, \langle x_2, 0.2e^{\iota\pi(0.1)}, 0.2e^{\iota\pi(0.1)}, 0.8e^{\iota\pi(0.7)} \rangle, \\ \langle x_3, 0.1e^{\iota\pi(0.1)}, 0.1e^{\iota\pi(0.1)}, 0.5e^{\iota\pi(0.4)} \rangle, \langle x_4, 0.2e^{\iota\pi(0.1)}, 0.2e^{\iota\pi(0.2)}, 0.4e^{\iota\pi(0.4)} \rangle \\ \mathfrak{e}_2 = \langle x_1, 0.3e^{\iota\pi(0.2)}, 0.3e^{\iota\pi(0.3)}, 0.8e^{\iota\pi(0.7)} \rangle, \langle x_2, 0.2e^{\iota\pi(0.1)}, 0.2e^{\iota\pi(0.1)}, 0.8e^{\iota\pi(0.7)} \rangle, \\ \langle x_3, 0.1e^{\iota\pi(0.1)}, 0.1e^{\iota\pi(0.1)}, 0.5e^{\iota\pi(0.4)} \rangle, \langle x_4, 0.2e^{\iota\pi(0.1)}, 0.2e^{\iota\pi(0.2)}, 0.4e^{\iota\pi(0.3)} \rangle \end{bmatrix}$$

$$(\tilde{\mathcal{F}}_1, \tilde{\mathcal{E}}) \setminus (\tilde{\mathcal{F}}_2, \tilde{\mathcal{E}}) = \begin{bmatrix} \mathfrak{e}_1 = \langle x_1, 0.3e^{\iota\pi(0.2)}, 0.3e^{\iota\pi(0.2)}, 0.6e^{\iota\pi(0.5)} \rangle, \langle x_2, 0.4e^{\iota\pi(0.3)}, 0.2e^{\iota\pi(0.1)}, 0.8e^{\iota\pi(0.7)} \rangle, \\ \langle x_3, 0.4e^{\iota\pi(0.3)}, 0.1e^{\iota\pi(0.1)}, 0.5e^{\iota\pi(0.4)} \rangle, \langle x_4, 0.2e^{\iota\pi(0.1)}, 0.2e^{\iota\pi(0.1)}, 0.5e^{\iota\pi(0.4)} \rangle \\ \mathfrak{e}_2 = \langle x_1, 0.4e^{\iota\pi(0.3)}, 0.3e^{\iota\pi(0.2)}, 0.8e^{\iota\pi(0.7)} \rangle, \langle x_2, 0.3e^{\iota\pi(0.2)}, 0.2e^{\iota\pi(0.1)}, 0.4e^{\iota\pi(0.3)} \rangle, \\ \langle x_3, 0.3e^{\iota\pi(0.2)}, 0.2e^{\iota\pi(0.1)}, 0.7e^{\iota\pi(0.6)} \rangle, \langle x_4, 0.1e^{\iota\pi(0.1)}, 0.1e^{\iota\pi(0.1)}, 0.9e^{\iota\pi(0.8)} \rangle \end{bmatrix}$$

$$(\tilde{\mathcal{F}}_1, \tilde{\mathcal{E}}) \wedge (\tilde{\mathcal{F}}_2, \tilde{\mathcal{E}}) = \begin{bmatrix} (\mathfrak{e}_1, \mathfrak{e}_1) = \langle x_1, 0.3e^{\iota\pi(0.2)}, 0.3e^{\iota\pi(0.2)}, 0.8e^{\iota\pi(0.7)} \rangle, \langle x_2, 0.2e^{\iota\pi(0.1)}, 0.2e^{\iota\pi(0.1)}, 0.8e^{\iota\pi(0.7)} \rangle, \\ \langle x_3, 0.1e^{\iota\pi(0.1)}, 0.1e^{\iota\pi(0.1)}, 0.5e^{\iota\pi(0.4)} \rangle, \langle x_4, 0.2e^{\iota\pi(0.1)}, 0.2e^{\iota\pi(0.1)}, 0.4e^{\iota\pi(0.3)} \rangle \\ (\mathfrak{e}_1, \mathfrak{e}_2) = \langle x_1, 0.3e^{\iota\pi(0.2)}, 0.4e^{\iota\pi(0.3)}, 0.6e^{\iota\pi(0.5)} \rangle, \langle x_2, 0.4e^{\iota\pi(0.3)}, 0.2e^{\iota\pi(0.1)}, 0.8e^{\iota\pi(0.7)} \rangle, \\ \langle x_3, 0.5e^{\iota\pi(0.4)}, 0.2e^{\iota\pi(0.1)}, 0.5e^{\iota\pi(0.4)} \rangle, \langle x_4, 0.2e^{\iota\pi(0.1)}, 0.2e^{\iota\pi(0.1)}, 0.6e^{\iota\pi(0.5)} \rangle \\ (\mathfrak{e}_2, \mathfrak{e}_1) = \langle x_1, 0.4e^{\iota\pi(0.3)}, 0.3e^{\iota\pi(0.2)}, 0.8e^{\iota\pi(0.7)} \rangle, \langle x_2, 0.2e^{\iota\pi(0.1)}, 0.4e^{\iota\pi(0.3)}, 0.8e^{\iota\pi(0.7)} \rangle, \\ \langle x_3, 0.1e^{\iota\pi(0.1)}, 0.1e^{\iota\pi(0.1)}, 0.7e^{\iota\pi(0.6)} \rangle, \langle x_4, 0.1e^{\iota\pi(0.1)}, 0.2e^{\iota\pi(0.1)}, 0.9e^{\iota\pi(0.8)} \rangle \\ (\mathfrak{e}_2, \mathfrak{e}_2) = \langle x_1, 0.3e^{\iota\pi(0.2)}, 0.3e^{\iota\pi(0.2)}, 0.8e^{\iota\pi(0.7)} \rangle, \langle x_2, 0.2e^{\iota\pi(0.1)}, 0.2e^{\iota\pi(0.1)}, 0.8e^{\iota\pi(0.7)} \rangle, \\ \langle x_3, 0.1e^{\iota\pi(0.1)}, 0.1e^{\iota\pi(0.1)}, 0.5e^{\iota\pi(0.4)} \rangle, \langle x_4, 0.2e^{\iota\pi(0.1)}, 0.2e^{\iota\pi(0.1)}, 0.4e^{\iota\pi(0.3)} \rangle \end{bmatrix}$$

$$(\tilde{\mathcal{F}}_1, \dot{\mathcal{E}}) \vee (\tilde{\mathcal{F}}, \dot{\mathcal{E}}) = \begin{bmatrix} (\mathbf{e}_1, \mathbf{e}_1) = \langle x_1, 0.6e^{\iota\pi(0.5)}, 0.4e^{\iota\pi(0.3)}, 0.6e^{\iota\pi(0.5)} \rangle, \langle x_2, 0.4e^{\iota\pi(0.3)}, 0.5e^{\iota\pi(0.4)}, 0.8e^{\iota\pi(0.7)} \rangle, \\ \langle x_3, 0.6e^{\iota\pi(0.5)}, 0.2e^{\iota\pi(0.1)}, 0.4e^{\iota\pi(0.3)} \rangle, \langle x_4, 0.5e^{\iota\pi(0.4)}, 0.3e^{\iota\pi(0.2)}, 0.3e^{\iota\pi(0.2)} \rangle \\ (\mathbf{e}_1, \mathbf{e}_2) = \langle x_1, 0.7e^{\iota\pi(0.6)}, 0.5e^{\iota\pi(0.4)}, 0.8e^{\iota\pi(0.7)} \rangle, \langle x_2, 0.4e^{\iota\pi(0.3)}, 0.2e^{\iota\pi(0.1)}, 0.3e^{\iota\pi(0.2)} \rangle, \\ \langle x_3, 0.6e^{\iota\pi(0.5)}, 0.3e^{\iota\pi(0.2)}, 0.4e^{\iota\pi(0.3)} \rangle, \langle x_4, 0.4e^{\iota\pi(0.3)}, 0.3e^{\iota\pi(0.2)}, 0.4e^{\iota\pi(0.3)} \rangle \\ (\mathbf{e}_2, \mathbf{e}_1) = \langle x_1, 0.6e^{\iota\pi(0.5)}, 0.3e^{\iota\pi(0.2)}, 0.8e^{\iota\pi(0.7)} \rangle, \langle x_2, 0.3e^{\iota\pi(0.2)}, 0.5e^{\iota\pi(0.4)}, 0.2e^{\iota\pi(0.1)} \rangle, \\ \langle x_3, 0.3e^{\iota\pi(0.2)}, 0.2e^{\iota\pi(0.1)}, 0.4e^{\iota\pi(0.3)} \rangle, \langle x_4, 0.5e^{\iota\pi(0.4)}, 0.2e^{\iota\pi(0.1)}, 0.3e^{\iota\pi(0.2)} \rangle \\ (\mathbf{e}_2, \mathbf{e}_2) = \langle x_1, 0.7e^{\iota\pi(0.6)}, 0.5e^{\iota\pi(0.4)}, 0.6e^{\iota\pi(0.5)} \rangle, \langle x_2, 0.4e^{\iota\pi(0.3)}, 0.4e^{\iota\pi(0.3)}, 0.2e^{\iota\pi(0.1)} \rangle, \\ \langle x_3, 0.5e^{\iota\pi(0.4)}, 0.3e^{\iota\pi(0.2)}, 0.4e^{\iota\pi(0.3)} \rangle, \langle x_4, 0.4e^{\iota\pi(0.3)}, 0.2e^{\iota\pi(0.1)}, 0.6e^{\iota\pi(0.5)} \rangle \end{bmatrix}$$

4. Topological Spaces Based on Complex Neutrosophic Soft Sets

Based on the previously established operations of CNS union, intersection, and the neutrosophic soft null and absolute sets, the idea of a CNS topology is presented in this section. To improve comprehension of these ideas, illustrative examples are given.

Definition 14. The family of all CNS sets defined on \mathbb{X} and $\tau \subset \text{CNSS}(\mathbb{X}, \dot{\mathcal{E}})$ is represented by the CNS set $(\mathbb{X}, \dot{\mathcal{E}})$. The CNS topology on \mathbb{X} is therefore defined as τ if

- (i) $0_{(\mathbb{X}, \dot{\mathcal{E}})}$ and $1_{(\mathbb{X}, \dot{\mathcal{E}})} \in \tau$,
- (ii) If any number of CNS sets are taken from τ , their union also lies in τ ,
- (iii) If a finite number of CNS sets are taken from τ , then their intersection also lies in τ .

Then, a CNST space (CNSTS) over \mathbb{X} is defined as $(\mathbb{X}, \tau, \dot{\mathcal{E}})$. A CNS open set is defined for each element of τ .

Definition 15. The CNST space $(\mathbb{X}, \tau, \dot{\mathcal{E}})$ and the CNS set $(\tilde{\mathcal{F}}, \dot{\mathcal{E}})$ over \mathbb{X} are considered. If and only if its counterpart is a CNS open set, then $(\tilde{\mathcal{F}}, \dot{\mathcal{E}})$ is a CNS closed set.

Proposition 4. Consider the CNS spaces $(\mathbb{X}, \tau, \dot{\mathcal{E}})$ on \mathbb{X} . Next,

- (i) $0_{(\mathbb{X}, \dot{\mathcal{E}})}$ and $1_{(\mathbb{X}, \dot{\mathcal{E}})}$ are CNS closed sets over \mathbb{X} ,
- (ii) If any number of CNS closed sets are taken over \mathbb{X} , their union is itself a CNS closed set.
- (iii) If any number of CNS closed sets are taken over \mathbb{X} , their intersection is itself a CNS closed set.

Definition 16. The family of all CNS sets in the universe \mathbb{X} is represented by the CNS set $(\mathbb{X}, \dot{\mathcal{E}})$.

- (i) If $\tau = \{0_{(\mathbb{X}, \dot{\mathcal{E}})}, 1_{(\mathbb{X}, \dot{\mathcal{E}})}\}$, then τ is referred to as a CNS indiscrete topology, and $(\mathbb{X}, \tau, \dot{\mathcal{E}})$ is defined as a CNS indiscrete topological space over \mathbb{X} .
- (ii) If $\tau = \text{CNSS}(\mathbb{X}, \dot{\mathcal{E}})$, then τ is called a CNS discrete topology and $(\mathbb{X}, \tau, \dot{\mathcal{E}})$ is referred to as a CNS discrete topological space over \mathbb{X} .

Proposition 5. For the same universe \mathbb{X} , let $(\mathbb{X}, \tau_1, \dot{\mathcal{E}})$ and $(\mathbb{X}, \tau_2, \dot{\mathcal{E}})$ be CNST spaces. Then $(\mathbb{X}, \tau_1 \cap \tau_2, \dot{\mathcal{E}})$ is a CNST space over \mathbb{X} .

Proof. (i). Since $0_{(\mathbb{X}, \dot{\mathcal{E}})}, 1_{(\mathbb{X}, \dot{\mathcal{E}})} \in \tau_1$ and $0_{(\mathbb{X}, \dot{\mathcal{E}})}, 1_{(\mathbb{X}, \dot{\mathcal{E}})} \in \tau_2$, then $0_{(\mathbb{X}, \dot{\mathcal{E}})}, 1_{(\mathbb{X}, \dot{\mathcal{E}})} \in \tau_1 \cap \tau_2$.
(ii). Assume that $\{(\tilde{\mathcal{F}}_i, \dot{\mathcal{E}}) | i \in I\}$ be a collection of CNS sets in $\tau_1 \cap \tau_2$. Then $(\tilde{\mathcal{F}}_i, \dot{\mathcal{E}}) \in \tau_1$ and $(\tilde{\mathcal{F}}_i, \dot{\mathcal{E}}) \in \tau_2$ for all $i \in I$, so $\cup_{i \in I} (\tilde{\mathcal{F}}_i, \dot{\mathcal{E}}) \in \tau_1$ and $\cup_{i \in I} (\tilde{\mathcal{F}}_i, \dot{\mathcal{E}}) \in \tau_2$. Thus $\cup_{i \in I} (\tilde{\mathcal{F}}_i, \dot{\mathcal{E}}) \in \tau_1 \cap \tau_2$.
(iii). Suppose that $\{(\tilde{\mathcal{F}}_i, \dot{\mathcal{E}}) | i = \overline{1, n}\}$ denotes the collection of finite number of CNS sets in $\tau_1 \cap \tau_2$. So, $(\tilde{\mathcal{F}}_i, \dot{\mathcal{E}}) \in \tau_1$ and $(\tilde{\mathcal{F}}_i, \dot{\mathcal{E}}) \in \tau_2$ for all $i = \overline{1, n}$, so $\cap_{i=1}^n (\tilde{\mathcal{F}}_i, \dot{\mathcal{E}}) \in \tau_1$ and $\cap_{i=1}^n (\tilde{\mathcal{F}}_i, \dot{\mathcal{E}}) \in \tau_2$. Hence $\cap_{i=1}^n (\tilde{\mathcal{F}}_i, \dot{\mathcal{E}}) \in \tau_1 \cap \tau_2$.

Remark 1. A CNS topology over \mathbb{X} is not always the result of the union of two CNS topologies over \mathbb{X} .

Example 2. Assuming an initial universe set of $\mathbb{X} = \{x_1, x_2, x_3\}$, $\mathcal{E} = \{\mathfrak{e}_1, \mathfrak{e}_2\}$ be a collection of rules and:

$$\begin{aligned}\tau_1 &= \{0_{(\mathbb{X}, \mathcal{E})}, 1_{(\mathbb{X}, \mathcal{E})}, (\tilde{\mathcal{F}}_1, \mathcal{E}), (\tilde{\mathcal{F}}_2, \mathcal{E}), (\tilde{\mathcal{F}}_3, \mathcal{E})\}, \\ \tau_2 &= \{0_{(\mathbb{X}, \mathcal{E})}, 1_{(\mathbb{X}, \mathcal{E})}, (\tilde{\mathcal{F}}_2, \mathcal{E}), (\tilde{\mathcal{F}}_4, \mathcal{E})\}.\end{aligned}$$

are topologies over \mathbb{X} that are CNS. The CNS sets $(\tilde{\mathcal{F}}_1, \mathcal{E})$, $(\tilde{\mathcal{F}}_2, \mathcal{E})$, $(\tilde{\mathcal{F}}_3, \mathcal{E})$, and $(\tilde{\mathcal{F}}_4, \mathcal{E})$ are written as follows:

$$\begin{aligned}(\tilde{\mathcal{F}}_1, \mathcal{E}) &= \begin{bmatrix} \mathfrak{e}_1 = \langle x_1, 0.9e^{\iota\pi(0.9)}, 0.6e^{\iota\pi(0.8)}, 0.3e^{\iota\pi(0.5)} \rangle, \langle x_2, 0.7e^{\iota\pi(0.7)}, 0.6e^{\iota\pi(0.5)}, 0.5e^{\iota\pi(0.4)} \rangle \\ \langle x_3, 0.4e^{\iota\pi(0.3)}, 0.5e^{\iota\pi(0.2)}, 0.4e^{\iota\pi(0.2)} \rangle; \\ \mathfrak{e}_2 = \langle x_1, 0.7e^{\iota\pi(0.9)}, 0.3e^{\iota\pi(0.8)}, 0.4e^{\iota\pi(0.7)} \rangle, \langle x_2, 0.6e^{\iota\pi(0.5)}, 0.5e^{\iota\pi(0.7)}, 0.4e^{\iota\pi(0.2)} \rangle, \\ \langle x_3, 0.7e^{\iota\pi(0.8)}, 0.4e^{\iota\pi(0.4)}, 0.3e^{\iota\pi(0.4)} \rangle. \end{bmatrix} \\ (\tilde{\mathcal{F}}_2, \mathcal{E}) &= \begin{bmatrix} \mathfrak{e}_1 = \langle x_1, 0.7e^{\iota\pi(0.8)}, 0.5e^{\iota\pi(0.4)}, 0.5e^{\iota\pi(0.5)} \rangle, \langle x_2, 0.6e^{\iota\pi(0.4)}, 0.5e^{\iota\pi(0.5)}, 0.7e^{\iota\pi(0.6)} \rangle \\ \langle x_3, 0.3e^{\iota\pi(0.2)}, 0.4e^{\iota\pi(0.2)}, 0.6e^{\iota\pi(0.8)} \rangle; \\ \mathfrak{e}_2 = \langle x_1, 0.6e^{\iota\pi(0.6)}, 0.2e^{\iota\pi(0.6)}, 0.5e^{\iota\pi(0.7)} \rangle, \langle x_2, 0.5e^{\iota\pi(0.4)}, 0.4e^{\iota\pi(0.1)}, 0.6e^{\iota\pi(0.7)} \rangle, \\ \langle x_3, 0.4e^{\iota\pi(0.3)}, 0.3e^{\iota\pi(0.3)}, 0.5e^{\iota\pi(0.4)} \rangle. \end{bmatrix} \\ (\tilde{\mathcal{F}}_3, \mathcal{E}) &= \begin{bmatrix} \mathfrak{e}_1 = \langle x_1, 0.5e^{\iota\pi(0.6)}, 0.4e^{\iota\pi(0.2)}, 0.6e^{\iota\pi(0.5)} \rangle, \langle x_2, 0.4e^{\iota\pi(0.2)}, 0.3e^{\iota\pi(0.1)}, 0.7e^{\iota\pi(0.7)} \rangle \\ \langle x_3, 0.2e^{\iota\pi(0.1)}, 0.3e^{\iota\pi(0.2)}, 0.8e^{\iota\pi(0.9)} \rangle; \\ \mathfrak{e}_2 = \langle x_1, 0.4e^{\iota\pi(0.3)}, 0.2e^{\iota\pi(0.1)}, 0.6e^{\iota\pi(0.8)} \rangle, \langle x_2, 0.4e^{\iota\pi(0.3)}, 0.2e^{\iota\pi(0.1)}, 0.8e^{\iota\pi(0.9)} \rangle, \\ \langle x_3, 0.3e^{\iota\pi(0.2)}, 0.3e^{\iota\pi(0.1)}, 0.6e^{\iota\pi(0.5)} \rangle. \end{bmatrix} \\ (\tilde{\mathcal{F}}_4, \mathcal{E}) &= \begin{bmatrix} \mathfrak{e}_1 = \langle x_1, 0.6e^{\iota\pi(0.7)}, 0.3e^{\iota\pi(0.2)}, 0.2e^{\iota\pi(0.1)} \rangle, \langle x_2, 0.5e^{\iota\pi(0.4)}, 0.3e^{\iota\pi(0.3)}, 0.8e^{\iota\pi(0.9)} \rangle \\ \langle x_3, 0.2e^{\iota\pi(0.2)}, 0.3e^{\iota\pi(0.1)}, 0.9e^{\iota\pi(0.9)} \rangle; \\ \mathfrak{e}_2 = \langle x_1, 0.3e^{\iota\pi(0.3)}, 0.2e^{\iota\pi(0.1)}, 0.7e^{\iota\pi(0.8)} \rangle, \langle x_2, 0.4e^{\iota\pi(0.2)}, 0.1e^{\iota\pi(0.1)}, 0.9e^{\iota\pi(0.9)} \rangle, \\ \langle x_3, 0.2e^{\iota\pi(0.2)}, 0.2e^{\iota\pi(0.1)}, 0.7e^{\iota\pi(0.8)} \rangle. \end{bmatrix}\end{aligned}$$

Owing to the fact that $(\tilde{\mathcal{F}}_1, \mathcal{E}) \cup (\tilde{\mathcal{F}}_4, \mathcal{E}) \not\subseteq \tau_1 \cup \tau_2$, then $\tau_1 \cup \tau_2$ cannot be regarded as a CNS topology over \mathbb{X} .

Proposition 6. Consider the CNST space $(\mathbb{X}, \tau, \mathcal{E})$ over \mathbb{X} and

$$\tau = \{(\tilde{\mathcal{F}}_i, \mathcal{E}) : (\tilde{\mathcal{F}}_i, \mathcal{E}) \in \text{CNSS}(\mathbb{X}, \mathcal{E})\} = \{[e, \tilde{\mathcal{F}}_i(\mathfrak{e})]_{\mathfrak{e} \in \mathcal{E}} : (\tilde{\mathcal{F}}_i, \mathcal{E}) \in \text{CNSS}(\mathbb{X}, \mathcal{E})\}$$

where $\tilde{\mathcal{F}}_i(\mathfrak{e}) = \{\langle x, T_{\tilde{\mathcal{F}}_i(\mathfrak{e})}(x), I_{\tilde{\mathcal{F}}_i(\mathfrak{e})}(x), F_{\tilde{\mathcal{F}}_i(\mathfrak{e})}(x) \rangle : x \in \mathbb{X}\}$. Then

$$\begin{aligned}\tau_1 &= \{[T_{\tilde{\mathcal{F}}_i(\mathfrak{e})}(\mathbb{X})]_{\mathfrak{e} \in \mathcal{E}}\} \\ \tau_2 &= \{[I_{\tilde{\mathcal{F}}_i(\mathfrak{e})}(\mathbb{X})]_{\mathfrak{e} \in \mathcal{E}}\} \\ \tau_3 &= \{[F_{\tilde{\mathcal{F}}_i(\mathfrak{e})}(\mathbb{X})]_{\mathfrak{e} \in \mathcal{E}}\}\end{aligned}$$

describes fuzzy soft topologies that are complicated on \mathbb{X} .

Proof. (i). $0_{(\mathbb{X}, \mathcal{E})}, 1_{(\mathbb{X}, \mathcal{E})} \in \tau \Rightarrow 0, 1 \in \tau_1, 0, 1 \in \tau_2, 0, 1 \in \tau_3$ and $0, 1 \in \tau_4$. (ii). Consider $(\tilde{\mathcal{F}}_i, \mathcal{E}) | i \in I$ denotes the collection of CNS sets in τ . Then $\{[T_{\tilde{\mathcal{F}}_i(\mathfrak{e})}(\mathbb{X})]_{\mathfrak{e} \in \mathcal{E}}\}_{i \in I}$ is the collection

of complex fuzzy soft sets in τ_1 , $\{[I_{\tilde{F}_i(\mathfrak{e})}(\mathbb{X})]_{\mathfrak{e} \in \mathcal{E}}\}_{i \in I}$ is the collection of complex fuzzy soft sets in τ_2 , $\{[F_{\tilde{F}_i(\mathfrak{e})}(\mathbb{X})]_{\mathfrak{e} \in \mathcal{E}}\}_{i \in I}$ is a family of complex fuzzy soft sets in τ_3 . Since τ is a CNS topology, then $\mathbb{U}_{i \in I}(\tilde{F}_i, \mathcal{E}) \in \tau_1$. That is,

$$\mathbb{U}_{i \in I}(\tilde{F}_i, \mathcal{E}) = \{\langle \sup[T_{\tilde{F}_i(\mathfrak{e})}(\mathbb{X})]_{\mathfrak{e} \in \mathcal{E}}, \sup[I_{\tilde{F}_i(\mathfrak{e})}(\mathbb{X})]_{\mathfrak{e} \in \mathcal{E}}, \inf[F_{\tilde{F}_i(\mathfrak{e})}(\mathbb{X})]_{\mathfrak{e} \in \mathcal{E}} \rangle\}_{i \in I} \in \tau.$$

Hence,

$$\begin{aligned} &\{\sup[T_{\tilde{F}_i(\mathfrak{e})}(\mathbb{X})]_{\mathfrak{e} \in \mathcal{E}}\}_{i \in I} \in \tau_1 \\ &\{\sup[I_{\tilde{F}_i(\mathfrak{e})}(\mathbb{X})]_{\mathfrak{e} \in \mathcal{E}}\}_{i \in I} \in \tau_2 \\ &\{\inf[F_{\tilde{F}_i(\mathfrak{e})}(\mathbb{X})]_{\mathfrak{e} \in \mathcal{E}}\}_{i \in I} \in \tau_3. \end{aligned}$$

(iii). Let $\{(\tilde{F}_i, \mathcal{E}) | i = \overline{1, n}\}$ represents a family of finite number of CNS sets in τ .

Then $\{[T_{\tilde{F}_i(\mathfrak{e})}(\mathbb{X})]_{\mathfrak{e} \in \mathcal{E}}\}_{i = \overline{1, n}}$ is a family of complex fuzzy soft sets in τ_1 , $\{[I_{\tilde{F}_i(\mathfrak{e})}(\mathbb{X})]_{\mathfrak{e} \in \mathcal{E}}\}_{i = \overline{1, n}}$ is a family of complex fuzzy soft sets in τ_2 , $\{[F_{\tilde{F}_i(\mathfrak{e})}(\mathbb{X})]_{\mathfrak{e} \in \mathcal{E}}\}_{i = \overline{1, n}}$ is a family of complex fuzzy soft sets in τ_3 . Since τ is a CNS topology, then $\mathbb{M}_{i=1}^n(\tilde{F}_i, \mathcal{E}) \in \tau_1$. That is,

$$\mathbb{M}_{i=1}^n(\tilde{F}_i, \mathcal{E}) = \{\langle \min[T_{\tilde{F}_i(\mathfrak{e})}(\mathbb{X})]_{\mathfrak{e} \in \mathcal{E}}, \min[I_{\tilde{F}_i(\mathfrak{e})}(\mathbb{X})]_{\mathfrak{e} \in \mathcal{E}}, \max[F_{\tilde{F}_i(\mathfrak{e})}(\mathbb{X})]_{\mathfrak{e} \in \mathcal{E}} \rangle\}_{i = \overline{1, n}} \in \tau.$$

Therefore,

$$\begin{aligned} &\{\min[T_{\tilde{F}_i(\mathfrak{e})}(\mathbb{X})]_{\mathfrak{e} \in \mathcal{E}}\}_{i \in I} \in \tau_1 \\ &\{\min[I_{\tilde{F}_i(\mathfrak{e})}(\mathbb{X})]_{\mathfrak{e} \in \mathcal{E}}\}_{i \in I} \in \tau_2 \\ &\{\min[F_{\tilde{F}_i(\mathfrak{e})}(\mathbb{X})]_{\mathfrak{e} \in \mathcal{E}}^c\}_{i \in I} \in \tau_3. \end{aligned}$$

Remark 2. In general, the converse of the above proposition does not hold.

Example 3. Let $\mathbb{X} = \{x_1, x_2, x_3\}$ be an initial universe set, $\mathcal{E} = \{\mathfrak{e}_1, \mathfrak{e}_2\}$ be a parameters set and:

$$\tau_1 = \{0_{(\mathbb{X}, \mathcal{E})}, 1_{(\mathbb{X}, \mathcal{E})}, (\tilde{F}_1, \mathcal{E}), (\tilde{F}_2, \mathcal{E}), (\tilde{F}_3, \mathcal{E})\}$$

be a family of CNS sets over \mathbb{X} . Here, the CNS sets $(\tilde{F}_1, \mathcal{E})$, $(\tilde{F}_2, \mathcal{E})$ and $(\tilde{F}_3, \mathcal{E})$ are mathematically defined as follows:

$$\begin{aligned} (\tilde{F}_1, \mathcal{E}) &= \begin{bmatrix} \mathfrak{e}_1 = \langle x_1, 0.9e^{\iota\pi(0.9)}, 0.6e^{\iota\pi(0.8)}, 0.3e^{\iota\pi(0.7)} \rangle, \langle x_2, 0.7e^{\iota\pi(0.7)}, 0.6e^{\iota\pi(0.5)}, 0.5e^{\iota\pi(0.4)} \rangle \\ \langle x_3, 0.4e^{\iota\pi(0.3)}, 0.5e^{\iota\pi(0.2)}, 0.4e^{\iota\pi(0.2)} \rangle; \\ \mathfrak{e}_2 = \langle x_1, 0.7e^{\iota\pi(0.9)}, 0.3e^{\iota\pi(0.8)}, 0.4e^{\iota\pi(0.7)} \rangle, \langle x_2, 0.6e^{\iota\pi(0.5)}, 0.5e^{\iota\pi(0.7)}, 0.4e^{\iota\pi(0.2)} \rangle, \\ \langle x_3, 0.7e^{\iota\pi(0.8)}, 0.4e^{\iota\pi(0.4)}, 0.3e^{\iota\pi(0.4)} \rangle. \end{bmatrix} \\ (\tilde{F}_2, \mathcal{E}) &= \begin{bmatrix} \mathfrak{e}_1 = \langle x_1, 0.7e^{\iota\pi(0.8)}, 0.5e^{\iota\pi(0.4)}, 0.5e^{\iota\pi(0.8)} \rangle, \langle x_2, 0.6e^{\iota\pi(0.4)}, 0.5e^{\iota\pi(0.5)}, 0.7e^{\iota\pi(0.6)} \rangle \\ \langle x_3, 0.3e^{\iota\pi(0.2)}, 0.4e^{\iota\pi(0.2)}, 0.6e^{\iota\pi(0.8)} \rangle; \\ \mathfrak{e}_2 = \langle x_1, 0.6e^{\iota\pi(0.6)}, 0.2e^{\iota\pi(0.6)}, 0.5e^{\iota\pi(0.8)} \rangle, \langle x_2, 0.5e^{\iota\pi(0.4)}, 0.4e^{\iota\pi(0.1)}, 0.6e^{\iota\pi(0.7)} \rangle, \\ \langle x_3, 0.4e^{\iota\pi(0.3)}, 0.3e^{\iota\pi(0.3)}, 0.5e^{\iota\pi(0.4)} \rangle. \end{bmatrix} \\ (\tilde{F}_3, \mathcal{E}) &= \begin{bmatrix} \mathfrak{e}_1 = \langle x_1, 0.8e^{\iota\pi(0.8)}, 0.4e^{\iota\pi(0.2)}, 0.6e^{\iota\pi(0.8)} \rangle, \langle x_2, 0.4e^{\iota\pi(0.2)}, 0.3e^{\iota\pi(0.1)}, 0.7e^{\iota\pi(0.7)} \rangle \\ \langle x_3, 0.2e^{\iota\pi(0.1)}, 0.3e^{\iota\pi(0.2)}, 0.8e^{\iota\pi(0.9)} \rangle; \\ \mathfrak{e}_2 = \langle x_1, 0.4e^{\iota\pi(0.3)}, 0.2e^{\iota\pi(0.1)}, 0.6e^{\iota\pi(0.8)} \rangle, \langle x_2, 0.4e^{\iota\pi(0.3)}, 0.2e^{\iota\pi(0.1)}, 0.8e^{\iota\pi(0.9)} \rangle, \\ \langle x_3, 0.3e^{\iota\pi(0.2)}, 0.3e^{\iota\pi(0.1)}, 0.6e^{\iota\pi(0.5)} \rangle. \end{bmatrix} \end{aligned}$$

Then,

$$\begin{aligned}\tau_1 &= \{\langle T_{\tilde{\mathcal{F}}_0(\mathbb{X}, \mathcal{E})(\mathfrak{e})}(\mathbb{X}), T_{\tilde{\mathcal{F}}_1(\mathbb{X}, \mathcal{E})(\mathfrak{e})}(\mathbb{X}), T_{\tilde{\mathcal{F}}_1(\mathfrak{e})}(\mathbb{X}), T_{\tilde{\mathcal{F}}_2(\mathfrak{e})}(\mathbb{X}), T_{\tilde{\mathcal{F}}_3(\mathfrak{e})}(\mathbb{X}) \rangle_{\mathfrak{e} \in \mathcal{E}}\}, \\ \tau_2 &= \{\langle I_{\tilde{\mathcal{F}}_0(\mathbb{X}, \mathcal{E})(\mathfrak{e})}(\mathbb{X}), I_{\tilde{\mathcal{F}}_1(\mathbb{X}, \mathcal{E})(\mathfrak{e})}(\mathbb{X}), I_{\tilde{\mathcal{F}}_1(\mathfrak{e})}(\mathbb{X}), I_{\tilde{\mathcal{F}}_2(\mathfrak{e})}(\mathbb{X}), I_{\tilde{\mathcal{F}}_3(\mathfrak{e})}(\mathbb{X}) \rangle_{\mathfrak{e} \in \mathcal{E}}\}, \\ \tau_3 &= \{\langle F_{\tilde{\mathcal{F}}_0(\mathbb{X}, \mathcal{E})(\mathfrak{e})}(\mathbb{X}), F_{\tilde{\mathcal{F}}_1(\mathbb{X}, \mathcal{E})(\mathfrak{e})}(\mathbb{X}), F_{\tilde{\mathcal{F}}_1(\mathfrak{e})}(\mathbb{X}), F_{\tilde{\mathcal{F}}_2(\mathfrak{e})}(\mathbb{X}), F_{\tilde{\mathcal{F}}_3(\mathfrak{e})}(\mathbb{X}) \rangle_{\mathfrak{e} \in \mathcal{E}}\}.\end{aligned}$$

are complex fuzzy soft topologies on \mathbb{X} . For example,

$$\begin{aligned}\tau_1 &= \{\langle (0, 0, 0), (1, 1, 1), (0.9e^{\iota\pi(0.9)}, 0.7e^{\iota\pi(0.7)}, 0.4e^{\iota\pi(0.3)}), \\ &\quad (0.7e^{\iota\pi(0.8)}, 0.6e^{\iota\pi(0.4)}, 0.3e^{\iota\pi(0.2)}), (0.8e^{\iota\pi(0.8)}, 0.4e^{\iota\pi(0.2)}, 0.2e^{\iota\pi(0.1)}) \rangle_{\mathfrak{e}_1}, \\ &\quad \langle (0, 0, 0), (1, 1, 1), (0.7e^{\iota\pi(0.9)}, 0.6e^{\iota\pi(0.5)}, 0.7e^{\iota\pi(0.8)}), \\ &\quad (0.6e^{\iota\pi(0.6)}, 0.5e^{\iota\pi(0.4)}, 0.4e^{\iota\pi(0.3)}), (0.4e^{\iota\pi(0.3)}, 0.4e^{\iota\pi(0.3)}, 0.3e^{\iota\pi(0.2)}) \rangle_{\mathfrak{e}_2}\}\end{aligned}$$

$$\begin{aligned}\tau_2 &= \{\langle (0, 0, 0), (1, 1, 1), (0.6e^{\iota\pi(0.8)}, 0.6e^{\iota\pi(0.5)}, 0.5e^{\iota\pi(0.2)}), \\ &\quad (0.5e^{\iota\pi(0.4)}, 0.5e^{\iota\pi(0.5)}, 0.4e^{\iota\pi(0.2)}), (0.4e^{\iota\pi(0.2)}, 0.3e^{\iota\pi(0.1)}, 0.3e^{\iota\pi(0.2)}) \rangle_{\mathfrak{e}_1}, \\ &\quad \langle (0, 0, 0), (1, 1, 1), (0.3e^{\iota\pi(0.8)}, 0.5e^{\iota\pi(0.7)}, 0.4e^{\iota\pi(0.4)}), \\ &\quad (0.2e^{\iota\pi(0.6)}, 0.4e^{\iota\pi(0.1)}, 0.3e^{\iota\pi(0.3)}), (0.2e^{\iota\pi(0.1)}, 0.2e^{\iota\pi(0.1)}, 0.3e^{\iota\pi(0.1)}) \rangle_{\mathfrak{e}_2}\}\end{aligned}$$

$$\begin{aligned}\tau_3 &= \{\langle (0, 0, 0), (1, 1, 1), (0.3e^{\iota\pi(0.7)}, 0.5e^{\iota\pi(0.4)}, 0.4e^{\iota\pi(0.2)}), \\ &\quad (0.5e^{\iota\pi(0.8)}, 0.7e^{\iota\pi(0.6)}, 0.6e^{\iota\pi(0.8)}), (0.6e^{\iota\pi(0.8)}, 0.7e^{\iota\pi(0.7)}, 0.8e^{\iota\pi(0.9)}) \rangle_{\mathfrak{e}_1}, \\ &\quad \langle (0, 0, 0), (1, 1, 1), (0.4e^{\iota\pi(0.7)}, 0.4e^{\iota\pi(0.2)}, 0.3e^{\iota\pi(0.4)}), \\ &\quad (0.5e^{\iota\pi(0.8)}, 0.6e^{\iota\pi(0.7)}, 0.5e^{\iota\pi(0.4)}), (0.6e^{\iota\pi(0.8)}, 0.8e^{\iota\pi(0.9)}, 0.6e^{\iota\pi(0.5)}) \rangle_{\mathfrak{e}_2}\}\end{aligned}$$

Since $(\tilde{\mathcal{F}}_2, \mathcal{E}) \cap (\tilde{\mathcal{F}}_3, \mathcal{E}) \notin \tau$, τ is not a CNS topology on \mathbb{X} .

Proposition 7. Let $(\mathbb{X}, \tau, \mathcal{E})$ be a CNST space over \mathbb{X} . Then

$$\begin{aligned}\tau_{1\mathfrak{e}} &= \{[T_{\tilde{\mathcal{F}}(\mathfrak{e})}(\mathbb{X})] : \tilde{\mathcal{F}}, \mathcal{E} \in \tau\} \\ \tau_{2\mathfrak{e}} &= \{[I_{\tilde{\mathcal{F}}(\mathfrak{e})}(\mathbb{X})] : \tilde{\mathcal{F}}, \mathcal{E} \in \tau\} \\ \tau_{3\mathfrak{e}} &= \{[F_{\tilde{\mathcal{F}}(\mathfrak{e})}(\mathbb{X})] : \tilde{\mathcal{F}}, \mathcal{E} \in \tau\}\end{aligned}$$

for all $\mathfrak{e} \in \mathcal{E}$ defines complex fuzzy topologies on \mathbb{X} .

Remark 3. The converse need not hold

Example 4. Consider the Example 3. Then,

$$\begin{aligned}\tau_{1\mathfrak{e}_1} &= \{\langle T_{\tilde{\mathcal{F}}_0(\mathbb{X}, \mathcal{E})(\mathfrak{e}_1)}(\mathbb{X}), T_{\tilde{\mathcal{F}}_1(\mathbb{X}, \mathcal{E})(\mathfrak{e}_1)}(\mathbb{X}), T_{\tilde{\mathcal{F}}_1(\mathfrak{e}_1)}(\mathbb{X}), T_{\tilde{\mathcal{F}}_2(\mathfrak{e}_1)}(\mathbb{X}), T_{\tilde{\mathcal{F}}_3(\mathfrak{e}_1)}(\mathbb{X}) \rangle\}, \\ \tau_{2\mathfrak{e}_1} &= \{\langle I_{\tilde{\mathcal{F}}_0(\mathbb{X}, \mathcal{E})(\mathfrak{e}_1)}(\mathbb{X}), I_{\tilde{\mathcal{F}}_1(\mathbb{X}, \mathcal{E})(\mathfrak{e}_1)}(\mathbb{X}), I_{\tilde{\mathcal{F}}_1(\mathfrak{e}_1)}(\mathbb{X}), I_{\tilde{\mathcal{F}}_2(\mathfrak{e}_1)}(\mathbb{X}), I_{\tilde{\mathcal{F}}_3(\mathfrak{e}_1)}(\mathbb{X}) \rangle\}, \\ \tau_{3\mathfrak{e}_1} &= \{\langle F_{\tilde{\mathcal{F}}_0(\mathbb{X}, \mathcal{E})(\mathfrak{e}_1)}(\mathbb{X}), F_{\tilde{\mathcal{F}}_1(\mathbb{X}, \mathcal{E})(\mathfrak{e}_1)}(\mathbb{X}), F_{\tilde{\mathcal{F}}_1(\mathfrak{e}_1)}(\mathbb{X}), F_{\tilde{\mathcal{F}}_2(\mathfrak{e}_1)}(\mathbb{X}), F_{\tilde{\mathcal{F}}_3(\mathfrak{e}_1)}(\mathbb{X}) \rangle\}.\end{aligned}$$

are complex fuzzy soft topologies on \mathbb{X} . For example,

$$\tau_{1_{\epsilon_1}} = \{ \langle (0, 0, 0), (1, 1, 1), (0.9e^{\iota\pi(0.9)}, 0.7e^{\iota\pi(0.7)}, 0.4e^{\iota\pi(0.3)}), \\ (0.7e^{\iota\pi(0.8)}, 0.6e^{\iota\pi(0.4)}, 0.3e^{\iota\pi(0.2)}), (0.8e^{\iota\pi(0.8)}, 0.4e^{\iota\pi(0.2)}, 0.2e^{\iota\pi(0.1)}) \rangle \}$$

$$\tau_{2_{\epsilon_1}} = \{ \langle (0, 0, 0), (1, 1, 1), (0.6e^{\iota\pi(0.8)}, 0.6e^{\iota\pi(0.5)}, 0.5e^{\iota\pi(0.2)}), \\ (0.5e^{\iota\pi(0.4)}, 0.5e^{\iota\pi(0.5)}, 0.4e^{\iota\pi(0.2)}), (0.4e^{\iota\pi(0.2)}, 0.3e^{\iota\pi(0.1)}, 0.3e^{\iota\pi(0.2)}) \rangle \}$$

$$\tau_{3_{\epsilon_1}} = \{ \langle (0, 0, 0), (1, 1, 1), (0.3e^{\iota\pi(0.7)}, 0.5e^{\iota\pi(0.4)}, 0.4e^{\iota\pi(0.2)}), \\ (0.5e^{\iota\pi(0.8)}, 0.7e^{\iota\pi(0.6)}, 0.6e^{\iota\pi(0.8)}), (0.6e^{\iota\pi(0.8)}, 0.7e^{\iota\pi(0.7)}, 0.8e^{\iota\pi(0.9)}) \rangle \}$$

Here, $\{\tau_{1_{\epsilon_1}}, \tau_{2_{\epsilon_1}}, \tau_{3_{\epsilon_1}}\}$ and $\{\tau_{1_{\epsilon_2}}, \tau_{2_{\epsilon_2}}, \tau_{3_{\epsilon_2}}\}$ are complex fuzzy quadri-topology on \mathbb{X} . But τ is not a CNS topology on \mathbb{X} .

Definition 17. Let $(\mathbb{X}, \tau, \mathcal{E})$ be a CNSTspace over \mathbb{X} and $(\tilde{\mathcal{F}}, \mathcal{E}) \in \text{CNSS}(\mathbb{X}, \mathcal{E})$ be a CNS set. Then, the CNS interior of $(\tilde{\mathcal{F}}, \mathcal{E})$, represented by $(\tilde{\mathcal{F}}, \mathcal{E})^\circ$ is referred to as the neutrosophic soft union of all CNS open subsets of $(\tilde{\mathcal{F}}, \mathcal{E})$.

Clearly $(\tilde{\mathcal{F}}, \mathcal{E})^\circ$ is the greatest CNS open subset contained within $(\tilde{\mathcal{F}}, \mathcal{E})$.

Example 5. The CNS topology is considered as τ_1 given in Example 2. Assume that an any $(\tilde{\mathcal{F}}, \mathcal{E}) \in \text{CNSS}(\mathbb{X}, \mathcal{E})$ is expressed as following:

$$(\tilde{\mathcal{F}}, \mathcal{E}) = \left[\begin{array}{l} \epsilon_1 = \langle x_1, 0.8e^{\iota\pi(0.9)}, 0.6e^{\iota\pi(0.8)}, 0.4e^{\iota\pi(0.3)} \rangle, \langle x_2, 0.7e^{\iota\pi(0.6)}, 0.9e^{\iota\pi(0.8)}, 0.3e^{\iota\pi(0.2)} \rangle \\ \langle x_3, 0.5e^{\iota\pi(0.3)}, 0.6e^{\iota\pi(0.7)}, 0.3e^{\iota\pi(0.2)} \rangle; \\ \epsilon_2 = \langle x_1, 0.8e^{\iota\pi(0.7)}, 0.7e^{\iota\pi(0.6)}, 0.2e^{\iota\pi(0.3)} \rangle, \langle x_2, 0.9e^{\iota\pi(0.7)}, 0.7e^{\iota\pi(0.7)}, 0.4e^{\iota\pi(0.3)} \rangle, \\ \langle x_3, 0.8e^{\iota\pi(0.7)}, 0.5e^{\iota\pi(0.6)}, 0.4e^{\iota\pi(0.3)} \rangle. \end{array} \right]$$

Then $0_{(\mathbb{X}, \mathcal{E})}, (\tilde{\mathcal{F}}_2, \mathcal{E}), (\tilde{\mathcal{F}}_3, \mathcal{E}) \subseteq (\tilde{\mathcal{F}}, \mathcal{E})$. Therefore, $(\tilde{\mathcal{F}}, \mathcal{E})^\circ = 0_{(\mathbb{X}, \mathcal{E})} \cup (\tilde{\mathcal{F}}_2, \mathcal{E}) \cup (\tilde{\mathcal{F}}_3, \mathcal{E}) = (\tilde{\mathcal{F}}, \mathcal{E})$.

Theorem 1. Let $(\mathbb{X}, \tau, \mathcal{E})$ be a CNSTspace over \mathbb{X} and $(\tilde{\mathcal{F}}, \mathcal{E}) \in \text{CNSS}(\mathbb{X}, \mathcal{E})$. $(\tilde{\mathcal{F}}, \mathcal{E})$ is a CNS open set and iff $(\tilde{\mathcal{F}}, \mathcal{E}) = (\tilde{\mathcal{F}}, \mathcal{E})^\circ$.

Proof. Let $(\tilde{\mathcal{F}}, \mathcal{E})$ be a CNS open set. Then the largest CNS open set that is contained by $(\tilde{\mathcal{F}}, \mathcal{E})$ is equal to $(\tilde{\mathcal{F}}, \mathcal{E})$. Hence, $(\tilde{\mathcal{F}}, \mathcal{E}) = (\tilde{\mathcal{F}}, \mathcal{E})^\circ$. Conversely, it can be demonstrated that $(\tilde{\mathcal{F}}, \mathcal{E})^\circ$ is a CNS open set and if $(\tilde{\mathcal{F}}, \mathcal{E}) = (\tilde{\mathcal{F}}, \mathcal{E})^\circ$, then $(\tilde{\mathcal{F}}, \mathcal{E})$ is a CNS open set.

Theorem 2. Let $(\mathbb{X}, \tau, \mathcal{E})$ be a CNSTspace over \mathbb{X} and $(\tilde{\mathcal{F}}_1, \mathcal{E}), (\tilde{\mathcal{F}}_2, \mathcal{E}) \in \text{CNSS}(\mathbb{X}, \mathcal{E})$. Then,

- (i) $[(\tilde{\mathcal{F}}, \mathcal{E})^\circ]^\circ = (\tilde{\mathcal{F}}, \mathcal{E})^\circ$,
- (ii) $(0_{(\mathbb{X}, \mathcal{E})})^\circ = 0_{(\mathbb{X}, \mathcal{E})}$ and $(1_{(\mathbb{X}, \mathcal{E})})^\circ = 1_{(\mathbb{X}, \mathcal{E})}$,
- (iii) $(\tilde{\mathcal{F}}_1, \mathcal{E}) \subseteq (\tilde{\mathcal{F}}_2, \mathcal{E}) \Rightarrow (\tilde{\mathcal{F}}_1, \mathcal{E})^\circ \subseteq (\tilde{\mathcal{F}}_2, \mathcal{E})^\circ$,
- (iv) $[(\tilde{\mathcal{F}}_1, \mathcal{E}) \cap (\tilde{\mathcal{F}}_2, \mathcal{E})]^\circ = (\tilde{\mathcal{F}}_1, \mathcal{E})^\circ \cap (\tilde{\mathcal{F}}_2, \mathcal{E})^\circ$,
- (v) $(\tilde{\mathcal{F}}_1, \mathcal{E})^\circ \cup (\tilde{\mathcal{F}}_2, \mathcal{E})^\circ \subseteq [(\tilde{\mathcal{F}}_1, \mathcal{E}) \cup (\tilde{\mathcal{F}}_2, \mathcal{E})]^\circ$.

Proof.

(i) Let $(\tilde{\mathcal{F}}_1, \mathcal{E})^\circ = (\tilde{\mathcal{F}}_2, \mathcal{E})$ Then $(\tilde{\mathcal{F}}_2, \mathcal{E}) \in \tau$ if and only if $(\tilde{\mathcal{F}}_2, \mathcal{E}) = (\tilde{\mathcal{F}}_2, \mathcal{E})^\circ$. So $[(\tilde{\mathcal{F}}_1, \mathcal{E})^\circ]^\circ = (\tilde{\mathcal{F}}_1, \mathcal{E})^\circ$.

(ii) Since $0_{(\mathbb{X}, \mathcal{E})}$ and $1_{(\mathbb{X}, \mathcal{E})}$ which are always CNS open sets, therefore we have:

$$(0_{(\mathbb{X}, \mathcal{E})})^\circ = 0_{(\mathbb{X}, \mathcal{E})}, \quad \text{and} \quad (1_{(\mathbb{X}, \mathcal{E})})^\circ = 1_{(\mathbb{X}, \mathcal{E})}.$$

(iii) It can be shown that $(\tilde{\mathcal{F}}_1, \mathcal{E})^\circ \subseteq (\tilde{\mathcal{F}}_1, \mathcal{E}) \subseteq (\tilde{\mathcal{F}}_2, \mathcal{E})$ and $(\tilde{\mathcal{F}}_2, \mathcal{E})^\circ \subseteq (\tilde{\mathcal{F}}_2, \mathcal{E})$. Since $(\tilde{\mathcal{F}}_2, \mathcal{E})^\circ$ is the largest CNS open set contained in $(\tilde{\mathcal{F}}_2, \mathcal{E})$ and so $(\tilde{\mathcal{F}}_1, \mathcal{E})^\circ \subseteq (\tilde{\mathcal{F}}_2, \mathcal{E})^\circ$.

(iv) Given that $(\tilde{\mathcal{F}}_1, \mathcal{E}) \cap (\tilde{\mathcal{F}}_2, \mathcal{E}) \subseteq (\tilde{\mathcal{F}}_1, \mathcal{E})$ and $(\tilde{\mathcal{F}}_1, \mathcal{E}) \cap (\tilde{\mathcal{F}}_2, \mathcal{E}) \subseteq (\tilde{\mathcal{F}}_2, \mathcal{E})$, then $[(\tilde{\mathcal{F}}_1, \mathcal{E}) \cap (\tilde{\mathcal{F}}_2, \mathcal{E})]^\circ \subseteq (\tilde{\mathcal{F}}_1, \mathcal{E})^\circ$ and $[(\tilde{\mathcal{F}}_1, \mathcal{E}) \cap (\tilde{\mathcal{F}}_2, \mathcal{E})]^\circ \subseteq (\tilde{\mathcal{F}}_2, \mathcal{E})^\circ$ and so,

$$[(\tilde{\mathcal{F}}_1, \mathcal{E}) \cap (\tilde{\mathcal{F}}_2, \mathcal{E})]^\circ \subseteq (\tilde{\mathcal{F}}_1, \mathcal{E})^\circ \cap (\tilde{\mathcal{F}}_2, \mathcal{E})^\circ.$$

Alternatively, since $(\tilde{\mathcal{F}}_1, \mathcal{E})^\circ \subseteq (\tilde{\mathcal{F}}_1, \mathcal{E})$ and $(\tilde{\mathcal{F}}_2, \mathcal{E})^\circ \subseteq (\tilde{\mathcal{F}}_2, \mathcal{E})$, then:

$$(\tilde{\mathcal{F}}_1, \mathcal{E})^\circ \cap (\tilde{\mathcal{F}}_2, \mathcal{E})^\circ \subseteq (\tilde{\mathcal{F}}_1, \mathcal{E}) \cap (\tilde{\mathcal{F}}_2, \mathcal{E}).$$

Moreover, $[(\tilde{\mathcal{F}}_1, \mathcal{E}) \cap (\tilde{\mathcal{F}}_2, \mathcal{E})]^\circ \subseteq (\tilde{\mathcal{F}}_1, \mathcal{E}) \cap (\tilde{\mathcal{F}}_2, \mathcal{E})$ and is the largest CNS open set. As a result, $(\tilde{\mathcal{F}}_1, \mathcal{E})^\circ \cap (\tilde{\mathcal{F}}_2, \mathcal{E})^\circ \subseteq [(\tilde{\mathcal{F}}_1, \mathcal{E}) \cap (\tilde{\mathcal{F}}_2, \mathcal{E})]^\circ$. Thus, $[(\tilde{\mathcal{F}}_1, \mathcal{E}) \cap (\tilde{\mathcal{F}}_2, \mathcal{E})]^\circ = (\tilde{\mathcal{F}}_1, \mathcal{E})^\circ \cap (\tilde{\mathcal{F}}_2, \mathcal{E})^\circ$.

(v) As $(\tilde{\mathcal{F}}_1, \mathcal{E}) \subseteq (\tilde{\mathcal{F}}_1, \mathcal{E}) \cup (\tilde{\mathcal{F}}_2, \mathcal{E})$ and $(\tilde{\mathcal{F}}_2, \mathcal{E}) \subseteq (\tilde{\mathcal{F}}_1, \mathcal{E}) \cup (\tilde{\mathcal{F}}_2, \mathcal{E})$, then:

$$(\tilde{\mathcal{F}}_1, \mathcal{E})^\circ \subseteq [(\tilde{\mathcal{F}}_1, \mathcal{E}) \cup (\tilde{\mathcal{F}}_2, \mathcal{E})]^\circ, \quad \text{and} \quad (\tilde{\mathcal{F}}_2, \mathcal{E})^\circ \subseteq [(\tilde{\mathcal{F}}_1, \mathcal{E}) \cup (\tilde{\mathcal{F}}_2, \mathcal{E})]^\circ.$$

Therefore,

$$(\tilde{\mathcal{F}}_1, \mathcal{E})^\circ \cup (\tilde{\mathcal{F}}_2, \mathcal{E})^\circ \subseteq [(\tilde{\mathcal{F}}_1, \mathcal{E}) \cup (\tilde{\mathcal{F}}_2, \mathcal{E})]^\circ.$$

Definition 18. Suppose that $(\mathbb{X}, \tau, \mathcal{E})$ be a CNSTspace over \mathbb{X} and $(\tilde{\mathcal{F}}, \mathcal{E}) \in \text{CNSS}(\mathbb{X}, \mathcal{E})$ be a CNSS. Then, the CNS closure of $(\tilde{\mathcal{F}}, \mathcal{E})$, denoted by $\overline{(\tilde{\mathcal{F}}, \mathcal{E})}$ is given by the CNS intersection of all the CNS closed supersets of $(\tilde{\mathcal{F}}, \mathcal{E})$.

Clearly $\overline{(\tilde{\mathcal{F}}, \mathcal{E})}$ is the minimal CNS closed set that contains $(\tilde{\mathcal{F}}, \mathcal{E})$.

Example 6. Consider the CNS topology τ_1 given in Example 2. Assume that an any $(\tilde{\mathcal{F}}, \mathcal{E}) \in \text{CNSS}(\mathbb{X}, \mathcal{E})$ is defined as following:

$$(\tilde{\mathcal{F}}, \mathcal{E}) = \left[\begin{array}{l} \mathbf{e}_1 = \langle x_1, 0.2e^{\iota\pi(0.1)}, 0.3e^{\iota\pi(0.2)}, 0.9e^{\iota\pi(0.8)} \rangle, \langle x_2, 0.5e^{\iota\pi(0.4)}, 0.2e^{\iota\pi(0.1)}, 0.8e^{\iota\pi(0.8)} \rangle \\ \langle x_3, 0.2e^{\iota\pi(0.1)}, 0.2e^{\iota\pi(0.1)}, 0.7e^{\iota\pi(0.9)} \rangle; \\ \mathbf{e}_2 = \langle x_1, 0.1e^{\iota\pi(0.1)}, 0.2e^{\iota\pi(0.1)}, 0.8e^{\iota\pi(0.9)} \rangle, \langle x_2, 0.1e^{\iota\pi(0.1)}, 0.2e^{\iota\pi(0.1)}, 0.9e^{\iota\pi(0.8)} \rangle, \\ \langle x_3, 0.4e^{\iota\pi(0.3)}, 0.2e^{\iota\pi(0.1)}, 0.9e^{\iota\pi(0.9)} \rangle. \end{array} \right]$$

Evidently, $(0_{(\mathbb{X}, \mathcal{E})})^c, (1_{(\mathbb{X}, \mathcal{E})})^c, (\tilde{\mathcal{F}}_1, \mathcal{E})^c, (\tilde{\mathcal{F}}_2, \mathcal{E})^c$, and $(\tilde{\mathcal{F}}_3, \mathcal{E})^c$ are all CNS closed sets over (X, τ_1, E) . They are expressed as following:

$$(0_{(\mathbb{X}, \mathcal{E})})^c = 1_{(\mathbb{X}, \mathcal{E})}, \quad (1_{(\mathbb{X}, \mathcal{E})})^c = 0_{(\mathbb{X}, \mathcal{E})}$$

$$(\tilde{\mathcal{F}}_1, \mathcal{E})^c = \left[\begin{array}{l} \mathbf{e}_1 = \langle x_1, 0.9e^{\iota\pi(0.9)}, 0.4e^{\iota\pi(0.2)}, 0.3e^{\iota\pi(0.5)} \rangle, \langle x_2, 0.7e^{\iota\pi(0.7)}, 0.4e^{\iota\pi(0.5)}, 0.5e^{\iota\pi(0.4)} \rangle \\ \langle x_3, 0.4e^{\iota\pi(0.3)}, 0.5e^{\iota\pi(0.8)}, 0.4e^{\iota\pi(0.2)} \rangle; \\ \mathbf{e}_2 = \langle x_1, 0.7e^{\iota\pi(0.9)}, 0.7e^{\iota\pi(0.2)}, 0.4e^{\iota\pi(0.7)} \rangle, \langle x_2, 0.6e^{\iota\pi(0.5)}, 0.5e^{\iota\pi(0.3)}, 0.4e^{\iota\pi(0.2)} \rangle, \\ \langle x_3, 0.7e^{\iota\pi(0.8)}, 0.6e^{\iota\pi(0.6)}, 0.3e^{\iota\pi(0.4)} \rangle. \end{array} \right]$$

$$\begin{aligned}
(\tilde{\mathcal{F}}_2, \acute{\mathcal{E}})^c &= \begin{bmatrix} \mathbf{e}_1 = \langle \mathbf{x}_1, 0.7e^{\iota\pi(0.8)}, 0.5e^{\iota\pi(0.6)}, 0.5e^{\iota\pi(0.5)} \rangle, \langle \mathbf{x}_2, 0.6e^{\iota\pi(0.4)}, 0.5e^{\iota\pi(0.5)}, 0.7e^{\iota\pi(0.6)} \rangle \\ \langle \mathbf{x}_3, 0.3e^{\iota\pi(0.2)}, 0.6e^{\iota\pi(0.8)}, 0.6e^{\iota\pi(0.8)} \rangle; \\ \mathbf{e}_2 = \langle \mathbf{x}_1, 0.6e^{\iota\pi(0.6)}, 0.8e^{\iota\pi(0.4)}, 0.5e^{\iota\pi(0.7)} \rangle, \langle \mathbf{x}_2, 0.5e^{\iota\pi(0.4)}, 0.6e^{\iota\pi(0.9)}, 0.6e^{\iota\pi(0.7)} \rangle, \\ \langle \mathbf{x}_3, 0.4e^{\iota\pi(0.3)}, 0.7e^{\iota\pi(0.7)}, 0.5e^{\iota\pi(0.4)} \rangle. \end{bmatrix} \\
(\tilde{\mathcal{F}}_3, \acute{\mathcal{E}})^c &= \begin{bmatrix} \mathbf{e}_1 = \langle \mathbf{x}_1, 0.5e^{\iota\pi(0.6)}, 0.6e^{\iota\pi(0.8)}, 0.6e^{\iota\pi(0.5)} \rangle, \langle \mathbf{x}_2, 0.4e^{\iota\pi(0.2)}, 0.7e^{\iota\pi(0.9)}, 0.7e^{\iota\pi(0.7)} \rangle \\ \langle \mathbf{x}_3, 0.2e^{\iota\pi(0.1)}, 0.7e^{\iota\pi(0.8)}, 0.8e^{\iota\pi(0.9)} \rangle; \\ \mathbf{e}_2 = \langle \mathbf{x}_1, 0.4e^{\iota\pi(0.3)}, 0.8e^{\iota\pi(0.9)}, 0.6e^{\iota\pi(0.8)} \rangle, \langle \mathbf{x}_2, 0.4e^{\iota\pi(0.3)}, 0.8e^{\iota\pi(0.9)}, 0.8e^{\iota\pi(0.9)} \rangle, \\ \langle \mathbf{x}_3, 0.3e^{\iota\pi(0.2)}, 0.7e^{\iota\pi(0.9)}, 0.6e^{\iota\pi(0.5)} \rangle. \end{bmatrix}
\end{aligned}$$

Then $(1_{(\mathbb{X}, \acute{\mathcal{E}})})^c, (\tilde{\mathcal{F}}_1, \acute{\mathcal{E}})^c, (\tilde{\mathcal{F}}_2, \acute{\mathcal{E}})^c, (\tilde{\mathcal{F}}_3, \acute{\mathcal{E}})^c \supseteq (\tilde{\mathcal{F}}, \acute{\mathcal{E}})$. Therefore,

$$\overline{(\tilde{\mathcal{F}}, \acute{\mathcal{E}})} = (1_{(\mathbb{X}, \acute{\mathcal{E}})})^c \cap (\tilde{\mathcal{F}}_1, \acute{\mathcal{E}})^c \cap (\tilde{\mathcal{F}}_2, \acute{\mathcal{E}})^c \cap (\tilde{\mathcal{F}}_3, \acute{\mathcal{E}})^c = (\tilde{\mathcal{F}}_3, \acute{\mathcal{E}})^c$$

.

Theorem 3. Let $(\mathbb{X}, \tau, \acute{\mathcal{E}})$ be a CNSTspace over \mathbb{X} and $(\tilde{\mathcal{F}}, \acute{\mathcal{E}}) \in CNSS(\mathbb{X}, \acute{\mathcal{E}})$. $(\tilde{\mathcal{F}}, \acute{\mathcal{E}})$ is a CNS closed set if and only if $(\tilde{\mathcal{F}}, \acute{\mathcal{E}}) = \overline{(\tilde{\mathcal{F}}, \acute{\mathcal{E}})}$

Proof. Let $(\tilde{\mathcal{F}}, \acute{\mathcal{E}})$ be a CNS closed set. Then the smallest CNS open set that containing $(\tilde{\mathcal{F}}, \acute{\mathcal{E}})$ is equal to $(\tilde{\mathcal{F}}, \acute{\mathcal{E}})$. Hence, $(\tilde{\mathcal{F}}, \acute{\mathcal{E}}) = \overline{(\tilde{\mathcal{F}}, \acute{\mathcal{E}})}$

In contrast, it is given that $\overline{(\tilde{\mathcal{F}}, \acute{\mathcal{E}})}$ is a CNS closed set and if $(\tilde{\mathcal{F}}, \acute{\mathcal{E}}) = \overline{(\tilde{\mathcal{F}}, \acute{\mathcal{E}})}$, then $(\tilde{\mathcal{F}}, \acute{\mathcal{E}})$ is a CNS closed set.

Theorem 4. Suppose $(\mathbb{X}, \tau, \acute{\mathcal{E}})$ be a CNSTspace over \mathbb{X} and $(\tilde{\mathcal{F}}_1, \acute{\mathcal{E}}), (\tilde{\mathcal{F}}_2, \acute{\mathcal{E}}) \in CNSS(\mathbb{X}, \acute{\mathcal{E}})$. So,

- (i) $\overline{[(\tilde{\mathcal{F}}, \acute{\mathcal{E}})]} = \overline{(\tilde{\mathcal{F}}, \acute{\mathcal{E}})}$,
- (ii) $\overline{(0_{(\mathbb{X}, \acute{\mathcal{E}})})} = 0_{(\mathbb{X}, \acute{\mathcal{E}})}$ and $\overline{(1_{(\mathbb{X}, \acute{\mathcal{E}})})} = 1_{(\mathbb{X}, \acute{\mathcal{E}})}$,
- (iii) $(\tilde{\mathcal{F}}_1, \acute{\mathcal{E}}) \subseteq (\tilde{\mathcal{F}}_2, \acute{\mathcal{E}}) \Rightarrow \overline{(\tilde{\mathcal{F}}_1, \acute{\mathcal{E}})} \subseteq \overline{(\tilde{\mathcal{F}}_2, \acute{\mathcal{E}})}$,
- (iv) $\overline{[(\tilde{\mathcal{F}}_1, \acute{\mathcal{E}}) \cup (\tilde{\mathcal{F}}_2, \acute{\mathcal{E}})]} = \overline{(\tilde{\mathcal{F}}_1, \acute{\mathcal{E}})} \cup \overline{(\tilde{\mathcal{F}}_2, \acute{\mathcal{E}})}$,
- (v) $\overline{(\tilde{\mathcal{F}}_1, \acute{\mathcal{E}})} \cap \overline{(\tilde{\mathcal{F}}_2, \acute{\mathcal{E}})} \subseteq \overline{[(\tilde{\mathcal{F}}_1, \acute{\mathcal{E}}) \cap (\tilde{\mathcal{F}}_2, \acute{\mathcal{E}})]}$.

Proof.

- (i) Suppose $\overline{(\tilde{\mathcal{F}}_1, \acute{\mathcal{E}})} = (\tilde{\mathcal{F}}_2, \acute{\mathcal{E}})$ So $(\tilde{\mathcal{F}}_2, \acute{\mathcal{E}})$ a CNS closed set. Thus $(\tilde{\mathcal{F}}_2, \acute{\mathcal{E}})$ and $\overline{(\tilde{\mathcal{F}}_2, \acute{\mathcal{E}})}$ are equal. Therefore $\overline{[(\tilde{\mathcal{F}}_1, \acute{\mathcal{E}})]} = (\tilde{\mathcal{F}}_1, \acute{\mathcal{E}})$.

- (ii) Since $0_{(\mathbb{X}, \acute{\mathcal{E}})}$ and $1_{(\mathbb{X}, \acute{\mathcal{E}})}$ which are always CNS closed sets, therefore we have:

$$\overline{(0_{(\mathbb{X}, \acute{\mathcal{E}})})} = 0_{(\mathbb{X}, \acute{\mathcal{E}})}, \quad \text{and} \quad \overline{(1_{(\mathbb{X}, \acute{\mathcal{E}})})} = 1_{(\mathbb{X}, \acute{\mathcal{E}})}.$$

- (iii) It is Given that $(\tilde{\mathcal{F}}_1, \acute{\mathcal{E}}) \subseteq \overline{(\tilde{\mathcal{F}}_1, \acute{\mathcal{E}})}$ and $(\tilde{\mathcal{F}}_2, \acute{\mathcal{E}}) \subseteq \overline{(\tilde{\mathcal{F}}_2, \acute{\mathcal{E}})}$, so $(\tilde{\mathcal{F}}_1, \acute{\mathcal{E}}) \subseteq (\tilde{\mathcal{F}}_2, \acute{\mathcal{E}}) \subseteq \overline{(\tilde{\mathcal{F}}_2, \acute{\mathcal{E}})}$. Since $\overline{(\tilde{\mathcal{F}}_2, \acute{\mathcal{E}})}$ is the minimal CNS closed set that contains $(\tilde{\mathcal{F}}_1, \acute{\mathcal{E}})$, then $(\tilde{\mathcal{F}}_1, \acute{\mathcal{E}}) \subseteq (\tilde{\mathcal{F}}_2, \acute{\mathcal{E}})$.

- (iv) Since $(\tilde{\mathcal{F}}_1, \mathcal{E}) \subseteq (\tilde{\mathcal{F}}_1, \mathcal{E}) \sqcup (\tilde{\mathcal{F}}_2, \mathcal{E})$ and $(\tilde{\mathcal{F}}_2, \mathcal{E}) \subseteq (\tilde{\mathcal{F}}_1, \mathcal{E}) \sqcup (\tilde{\mathcal{F}}_2, \mathcal{E})$, then $\overline{(\tilde{\mathcal{F}}_1, \mathcal{E})} \subseteq \overline{[(\tilde{\mathcal{F}}_1, \mathcal{E}) \sqcup (\tilde{\mathcal{F}}_2, \mathcal{E})]}$ and $\overline{(\tilde{\mathcal{F}}_2, \mathcal{E})} \subseteq \overline{[(\tilde{\mathcal{F}}_1, \mathcal{E}) \sqcup (\tilde{\mathcal{F}}_2, \mathcal{E})]}$ and so,

$$\overline{(\tilde{\mathcal{F}}_1, \mathcal{E})} \sqcup \overline{(\tilde{\mathcal{F}}_2, \mathcal{E})} \subseteq \overline{[(\tilde{\mathcal{F}}_1, \mathcal{E}) \sqcup (\tilde{\mathcal{F}}_2, \mathcal{E})]}.$$

In contrast, it is known that $(\tilde{\mathcal{F}}_1, \mathcal{E}) \subseteq \overline{(\tilde{\mathcal{F}}_1, \mathcal{E})}$ and $(\tilde{\mathcal{F}}_2, \mathcal{E}) \subseteq \overline{(\tilde{\mathcal{F}}_2, \mathcal{E})}$, So:

$$(\tilde{\mathcal{F}}_1, \mathcal{E}) \sqcup (\tilde{\mathcal{F}}_2, \mathcal{E}) \subseteq \overline{(\tilde{\mathcal{F}}_1, \mathcal{E})} \sqcup \overline{(\tilde{\mathcal{F}}_2, \mathcal{E})}.$$

In addition, $\overline{[(\tilde{\mathcal{F}}_1, \mathcal{E}) \sqcup (\tilde{\mathcal{F}}_2, \mathcal{E})]}$ and is the smallest CNS closed set that containing $(\tilde{\mathcal{F}}_1, \mathcal{E}) \sqcup (\tilde{\mathcal{F}}_2, \mathcal{E})$. Hence, $\overline{[(\tilde{\mathcal{F}}_1, \mathcal{E}) \sqcup (\tilde{\mathcal{F}}_2, \mathcal{E})]} \subseteq \overline{(\tilde{\mathcal{F}}_1, \mathcal{E})} \sqcup \overline{(\tilde{\mathcal{F}}_2, \mathcal{E})}$. Therefore, $\overline{[(\tilde{\mathcal{F}}_1, \mathcal{E}) \sqcup (\tilde{\mathcal{F}}_2, \mathcal{E})]} = \overline{(\tilde{\mathcal{F}}_1, \mathcal{E})} \sqcup \overline{(\tilde{\mathcal{F}}_2, \mathcal{E})}$.

- (v) Since

$$(\tilde{\mathcal{F}}_1, \mathcal{E}) \cap (\tilde{\mathcal{F}}_2, \mathcal{E}) \subseteq \overline{[(\tilde{\mathcal{F}}_1, \mathcal{E}) \cap (\tilde{\mathcal{F}}_2, \mathcal{E})]}, \quad \text{and} \quad \overline{[(\tilde{\mathcal{F}}_1, \mathcal{E}) \cap (\tilde{\mathcal{F}}_2, \mathcal{E})]}$$

is the smallest CNS closed set that containing $(\tilde{\mathcal{F}}_1, \mathcal{E}) \cap (\tilde{\mathcal{F}}_2, \mathcal{E})$. Then,

$$\overline{[(\tilde{\mathcal{F}}_1, \mathcal{E}) \cap (\tilde{\mathcal{F}}_2, \mathcal{E})]} \subseteq \overline{(\tilde{\mathcal{F}}_1, \mathcal{E})} \cap \overline{(\tilde{\mathcal{F}}_2, \mathcal{E})}.$$

Theorem 5. Suppose $(\mathbb{X}, \tau, \mathcal{E})$ be a CNSTspace over \mathbb{X} , and suppose $(\tilde{\mathcal{F}}, \mathcal{E}) \in \text{CNSS}(\mathbb{X}, \mathcal{E})$. So:

$$(i) \quad \overline{[(\tilde{\mathcal{F}}, \mathcal{E})]^c} = [(\tilde{\mathcal{F}}, \mathcal{E})^c]^\circ,$$

$$(ii) \quad [(\tilde{\mathcal{F}}, \mathcal{E})^\circ]^c = \overline{[(\tilde{\mathcal{F}}, \mathcal{E})^c]}.$$

Proof.

- (i)

$$\begin{aligned} \overline{(\tilde{\mathcal{F}}, \mathcal{E})} &= \cap \{(\tilde{\mathcal{G}}, \mathcal{E}) \in \tau^c : (\tilde{\mathcal{G}}, \mathcal{E}) \supseteq (\tilde{\mathcal{F}}, \mathcal{E})\} \\ &\Rightarrow \overline{[(\tilde{\mathcal{F}}, \mathcal{E})]^c} = \left[\cap \{(\tilde{\mathcal{G}}, \mathcal{E}) \in \tau^c : (\tilde{\mathcal{G}}, \mathcal{E}) \supseteq (\tilde{\mathcal{F}}, \mathcal{E})\} \right]^c \\ &= \cup \{(\tilde{\mathcal{G}}, \mathcal{E})^c \in \tau : (\tilde{\mathcal{G}}, \mathcal{E})^c \subseteq (\tilde{\mathcal{F}}, \mathcal{E})^c\} \\ &= [(\tilde{\mathcal{F}}, \mathcal{E})^c]^\circ. \end{aligned}$$

- (ii)

$$\begin{aligned} (\tilde{\mathcal{F}}, \mathcal{E})^\circ &= \cup \{(\tilde{\mathcal{G}}, \mathcal{E}) \in \tau : (\tilde{\mathcal{G}}, \mathcal{E}) \subseteq (\tilde{\mathcal{F}}, \mathcal{E})\} \\ &\Rightarrow [(\tilde{\mathcal{F}}, \mathcal{E})^\circ]^c = \left[\cup \{(\tilde{\mathcal{G}}, \mathcal{E}) \in \tau : (\tilde{\mathcal{G}}, \mathcal{E}) \subseteq (\tilde{\mathcal{F}}, \mathcal{E})\} \right]^c \\ &= \cap \{(\tilde{\mathcal{G}}, \mathcal{E})^c \in \tau^c : (\tilde{\mathcal{G}}, \mathcal{E})^c \supseteq (\tilde{\mathcal{F}}, \mathcal{E})^c\} \\ &= \overline{[(\tilde{\mathcal{F}}, \mathcal{E})^c]}. \end{aligned}$$

5. Complex Neutrosophic Soft Set-Based Cotangent Similarity Approach for Multi-Source Signal Analysis

One analytical technique for determining how similar two vectors (data) are is the cotangent similarity measure (CSM). It is typically used in a wide range of applications related to machine learning, image processing, and data analysis. Additionally, by considering the geometry of the data points, CSM will be able to spot subtle patterns and associations that would have gone unnoticed in the absence of pure distance measurements. It is frequently used in data analysis, machine learning, and image processing. In a military operation, CMS can be used to classify potential targets based on surveillance data. This is accomplished by comparing a target's operational characteristics with previously established categorized profiles. The likelihood that the threats will be compared and classed appropriately is then high, and the degree to which a target fits inside pre-established threat designs is estimated. The classification and pattern recognition tasks are supported by several machine learning and visualization methods. Spline-Smoothed Curves in 3D Surface Plots, Grouped Bar Charts, 2D Pearson Correlation Heatmaps, and Sig 2D Cotangent Similarity Heatmaps.

5.1. Cotangent similarity measures

Let $T_i = (T_{ik}, I_{ik}, F_{ik})$, $C_j = (T_{jk}, I_{jk}, F_{jk})$ are two CNSSs. Each set is represented by three components for each feature k :

T_{ik} : Truth membership of feature k for T_i .

I_{ik} : Indeterminacy membership of feature k for T_i .

F_{ik} : Falsity-membership degree of feature k for T_i .

The values typically satisfy: $T_{ik}, I_{ik}, F_{ik} \in [0, 1]$

Similarly, for object C_j :

T_{jk} : Truth membership of feature k for C_j .

I_{jk} : Indeterminacy membership of feature k for C_j .

F_{jk} : Falsity-membership degree of feature k for C_j .

The values typically satisfy: $T_{jk}, I_{jk}, F_{jk} \in [0, 1]$.

The cotangent similarity measures between T_i and C_j is defined as:

$Cotangent_{CNSS}(T_i, C_j) =$

$$\frac{1}{n} \sum_{k=1}^n \left\{ \cot\left[\frac{\pi}{4} + \frac{\pi}{12} (|T_{ik} - T_{jk}| + |I_{ik} - I_{jk}| + |F_{ik} - F_{jk}|)\right] \right\}$$

5.2. Real-Time Military Target Classification with Cotangent Similarity and Advanced Surveillance Data Integration

Correctly identifying the target of operations $T = \{T_1, T_2, T_3\}$ using multi-source signal samples $S = \{S_1, S_2, S_3\}$ and correctly labeling them with their appropriate operational classifications $C = \{C_1, C_2, C_3\}$ is the primary challenge in modern surveillance and reconnaissance. Because of radar, thermal emission, electronic monitoring, and other signal detecting methods, the data on each target is ambiguous, imprecise, and diverse. This indeterminacy necessitates a mathematical procedure that can simultaneously accept untruth, indeterminacy, and truth. The multi-dimensional connection between the targets, signals, and classes with regard to event-based evaluations (e) and event-based measures is embodied in the operational classification matrix (Table 2).

Nevertheless, the straightforward comparison of raw signal response to targets and classes is unsuitable because of similarity values, unreliability and nonlinear correlation between attributes. To overcome this, the similarity measure between a target and a class, called Cotangent similarity measure, within the framework of the CNS set (Cotangent CNSS) is implemented, which permits measuring the similarity between any target-class pair. In both pairs (T_i, C_j) , the approach

uses the joint impact of truth-membership, indeterminacy-membership, and falsity-membership functions, which are normalized by $n=3$ attributes. This produces cotangent similarity scores which can be used to rank candidate target profiles comparatively with operational class templates.

Table 1: Matrix of Target Intelligence Features Based on Cotangent Similarity ($T \times S$)

	S_1	S_2	...	S_n
T_1	T_{11}, I_{11}, F_{11}	T_{12}, I_{12}, F_{12}	...	T_{1n}, I_{1n}, F_{1n}
T_2	T_{21}, I_{21}, F_{21}	T_{22}, I_{22}, F_{22}	...	T_{2n}, I_{2n}, F_{2n}
...
T_m	T_{m1}, I_{m1}, F_{m1}	T_{m2}, I_{m2}, F_{m2}	...	T_{mn}, I_{mn}, F_{mn}

The raw surveillance parameters for each target T_i , as gathered from each data source S_i , are displayed in this table 1. These are represented by the 3-dimensional feature vectors found in each cell, gives each target-source combination a thorough feature profile for preliminary analysis and threat modeling.

Table 2: Operational Classification Matrix for Target Surveillance Data ($T \times S \rightarrow C$)

Row-I	S_1	S_2	S_3	Row-II	C_1	C_2	C_3
T_1	$\begin{pmatrix} 0.5e^{\iota\pi(0.6)} \\ 0.7e^{\iota\pi(0.5)} \\ 0.3e^{\iota\pi(0.3)} \end{pmatrix}$	$\begin{pmatrix} 0.6e^{\iota\pi(0.7)} \\ 0.4e^{\iota\pi(0.4)} \\ 0.3e^{\iota\pi(0.4)} \end{pmatrix}$	$\begin{pmatrix} 0.3e^{\iota\pi(0.2)} \\ 0.5e^{\iota\pi(0.5)} \\ 0.8e^{\iota\pi(0.3)} \end{pmatrix}$	S_1	$\begin{pmatrix} 0.3e^{\iota\pi(0.4)} \\ 0.5e^{\iota\pi(0.7)} \\ 0.7e^{\iota\pi(0.7)} \end{pmatrix}$	$\begin{pmatrix} 0.7e^{\iota\pi(0.6)} \\ 0.6e^{\iota\pi(0.5)} \\ 0.2e^{\iota\pi(0.3)} \end{pmatrix}$	$\begin{pmatrix} 0.5e^{\iota\pi(0.8)} \\ 0.4e^{\iota\pi(0.7)} \\ 0.9e^{\iota\pi(0.3)} \end{pmatrix}$
T_2	$\begin{pmatrix} 0.4e^{\iota\pi(0.6)} \\ 0.7e^{\iota\pi(0.9)} \\ 0.5e^{\iota\pi(0.7)} \end{pmatrix}$	$\begin{pmatrix} 0.2e^{\iota\pi(0.4)} \\ 0.4e^{\iota\pi(0.9)} \\ 0.6e^{\iota\pi(0.3)} \end{pmatrix}$	$\begin{pmatrix} 0.7e^{\iota\pi(0.7)} \\ 0.4e^{\iota\pi(0.3)} \\ 0.6e^{\iota\pi(0.6)} \end{pmatrix}$	S_2	$\begin{pmatrix} 0.2e^{\iota\pi(0.5)} \\ 0.3e^{\iota\pi(0.2)} \\ 0.7e^{\iota\pi(0.3)} \end{pmatrix}$	$\begin{pmatrix} 0.6e^{\iota\pi(0.6)} \\ 0.7e^{\iota\pi(0.8)} \\ 0.4e^{\iota\pi(0.3)} \end{pmatrix}$	$\begin{pmatrix} 0.3e^{\iota\pi(0.6)} \\ 0.6e^{\iota\pi(0.7)} \\ 0.8e^{\iota\pi(0.9)} \end{pmatrix}$
T_3	$\begin{pmatrix} 0.7e^{\iota\pi(0.9)} \\ 0.6e^{\iota\pi(0.5)} \\ 0.8e^{\iota\pi(0.8)} \end{pmatrix}$	$\begin{pmatrix} 0.2e^{\iota\pi(0.4)} \\ 0.8e^{\iota\pi(0.5)} \\ 0.7e^{\iota\pi(0.6)} \end{pmatrix}$	$\begin{pmatrix} 0.6e^{\iota\pi(0.9)} \\ 0.3e^{\iota\pi(0.6)} \\ 0.2e^{\iota\pi(0.3)} \end{pmatrix}$	S_3	$\begin{pmatrix} 0.4e^{\iota\pi(0.4)} \\ 0.7e^{\iota\pi(0.5)} \\ 0.5e^{\iota\pi(0.9)} \end{pmatrix}$	$\begin{pmatrix} 0.6e^{\iota\pi(0.2)} \\ 0.3e^{\iota\pi(0.5)} \\ 0.4e^{\iota\pi(0.4)} \end{pmatrix}$	$\begin{pmatrix} 0.7e^{\iota\pi(0.2)} \\ 0.3e^{\iota\pi(0.8)} \\ 0.2e^{\iota\pi(0.3)} \end{pmatrix}$

This table 2 delineates the cotangent similarity values calculated by comparing the feature vectors of targets with those of established classified operational profiles (e.g., C_1 : high-value asset, C_2 : decoy, C_3 : communication node). The raw cosine similarity between each target (T) and its corresponding surveillance data (S) is presented in Row-I ($T \times S$). Meanwhile, the cotangent similarity between each data source vector and the classified operational profiles is displayed in Row-II ($S \times C$). This method facilitates the prioritization of actions (e.g., attack, monitor, ignore) by classifying or clustering targets according to their correlation with well-defined threat or operational categories.

All target-classification pairings are then averaged by adding the cotangent values that were determined for each pair of targets and categorized profiles.

The values of the resulting cotangent similarities are:

$$\text{Cotangent}_{CNSS}(T_1, C_1) = 0.4913$$

$$\text{Cotangent}_{CNSS}(T_1, C_2) = 0.6653$$

$$\text{Cotangent}_{CNSS}(T_1, C_3) = 0.5785$$

$$\text{Cotangent}_{CNSS}(T_2, C_1) = 0.5287$$

$$\text{Cotangent}_{CNSS}(T_2, C_2) = 0.4937$$

$$\text{Cotangent}_{CNSS}(T_2, C_3) = 0.3576$$

$$\text{Cotangent}_{CNSS}(T_3, C_1) = 0.4110$$

$$\text{Cotangent}_{CNSS}(T_3, C_2) = 0.4604$$

$$\text{Cotangent}_{CNSS}(T_3, C_3) = 0.4221.$$

Table 3: Cotangent Similarity scores between signal samples ($S_1 - S_3$) and class templates ($T_1 - T_3$)

Cot SM	S_1	S_2	S_3
T_1	0.4913	0.6653	0.5785
T_2	0.5287	0.4937	0.3576
T_3	0.4110	0.4604	0.4221

The degree to which each signal sample resembles the three class templates is shown in the cotangent similarity table 3. The template is most similar to S_1 , although the score is average in the case of S_1 , where the maximum similarity with T_2 is 0.5287. The highest match in S_2 with T_1 is 0.6653, which is also the highest value in the entire table. This indicates that S_2 is classified under template T_1 in a strong and reliable manner. The alignment with T_1 in S_3 has the highest similarity, at 0.5785, which falls within a moderate range and is not as definitive as S_2 . Overall, the results show that T_1 is capable of drawing in two signals, S_2 and S_3 , indicating that this template is a main or special active profile. Only S_1 is connected to T_2 , and their connection is not very strong. T_3 may be utilized as a weak or background category because it does not appear to be the best match to any signal and all of its scores are below the best ones. While S_1T_2 and S_3T_1 require closer interpretation or further investigation, S_2T_1 may be regarded as a specific classification in a realistic option.

6. Result and Discussion

Fig.1 was created using the Viridis colormap, which provides a smooth transition from dark purple to yellow, to create 2D Cotangent Similarity Matrix Heatmaps that show the degree of alignment between the input signals ($S_1 - S_3$) and the templates ($T_1 - T_3$). The highest similarity value, 0.66 (yellow), is also found in the $S_2 - T_1$ (0.6653) similarity. Since this circular region validates the strongest and most conclusive match in the matrix, Signal S_2 has the most reliable relationship with template T_1 . Strong similarity levels (0.57-0.58) are shown by $S_3 - T_1$ (0.5785) and $S_1 - T_2$ (0.5287), and their signal-template links are significant and dependable, indicating the potential for accurate categorization. Bluish-green (c. 0.4600-0.4920) matches, as those between $S_2 - T_2$ (0.4937) and $S_2 - T_3$ (0.4604), can be described as fairly equivalent; nonetheless, they are not as strong or definitive as the others, but they are still acceptable. Redder similarity regions, such as $S_1 - T_3$ (0.4110) and $S_3 - T_3$ (0.4221), are found in the blue to purple spectrum (0.41 -0.42). These are the weaker similarities that could need further research to validate. The most purple zone (< 0.40) is seen in $S_3 - T_2$ (0.3576), which indicates the lowest degree of similarity and the worst signal-template coupling. In general, Heatmaps offer a layered, visual depiction of how strong similarities are, with alignment confidence indicated by color intensity. This gives signal-to-template correlations a very clear and descriptive representation.

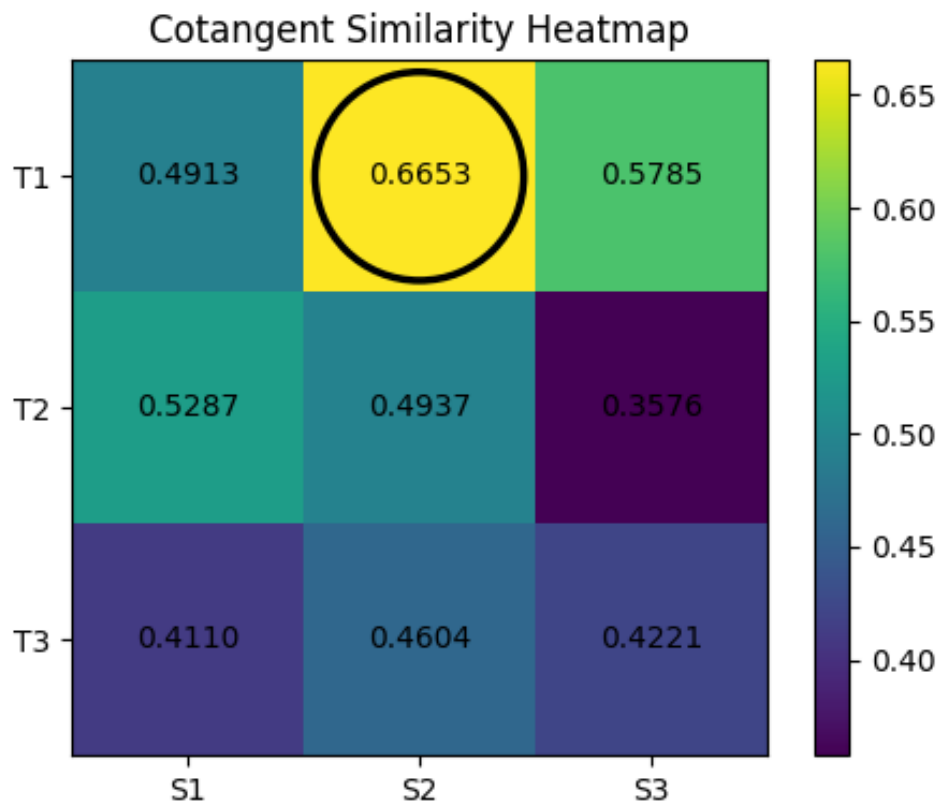


Figure 1

The Viridis colormap, which smoothly transitions from deep purple to green to yellow, is used in Fig.2 to generate normalized 2D Cotangent Similarity Heatmaps (minimum to maximum normalization along a row) that display the relative strength of alignment between signals ($S_1 - S_3$) and templates ($T_1 - T_3$). While the row with the weakest alignment is incredibly purple (about 0.000), the row with the closest resemblance is brilliant yellow (around 1.000). T_1S_2 (1.000), T_2S_1 (1.000), and T_3S_2 (1.000) are the most significant and authoritative pairs across the normalized matrix, and the most noticeable ones are surrounding. These findings show that signal S_2 shows a fairly consistent match with templates T_1 and T_3 , although template T_2 best matches signal S_1 . Although somewhat weaker than the row's maximum, Green (0.795) exhibits a close secondary similarity to T_2S_2 (0.795), making it a reasonably trustworthy match. Although teal-blue (e.g., T_1S_3 (0.501)) shows promise, the similarities are smaller and the signal-template relationship is less clear. The weaker ones are represented by the purple and dark-blue hues, such as T_3S_3 (0.225) and, more precisely, T_1S_1 (0.000), T_2S_3 (0.000), and T_3S_1 (0.000). These numbers show the least or no similarity between them in their respective rows. This normalized Heatmaps typically offers a more comparable view of the intra-row similarity distributions by showing the strongest matches (yellow) and preserving secondary and weaker ties to allow for a more comprehensive analysis.

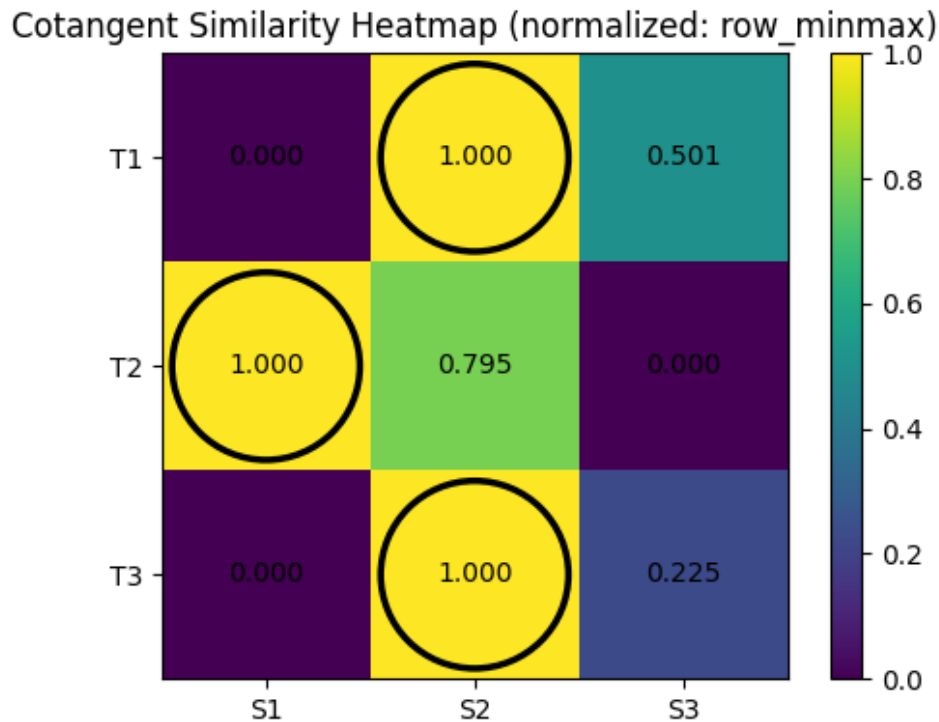


Figure 2

Fig.3 uses a red-blue color map that smoothly switches between deep blue (negative correlation), white (neutral), and deep red (positive correlation) to generate 2D Pearson Correlation Heat maps that show how signals ($S_1 - S_3$) interact with templates ($T_1 - T_3$). Deep blue ($= -0.97$) denotes a very strong negative link, while bright red ($= +0.87$) denotes a very strong positive correlation. The most significant link is made by a circle at T_2S_1 (0.87); hence, the positive association is highly consistent and aligned. Next is T_2S_2 (0.76), which is also a strong and significant positive correlation. Similar moderate positive correlations are shown by T_3S_1 (0.58) and T_2S_3 (0.42), suggesting fair but less dominant signal-template alignment. However, there are certain couples with very negative relationships. For instance, the highly substantial negative correlations between T_1S_3 (-0.97) and T_1S_2 (-0.78) imply that these signals are anti-phase to template T_1 . T_3S_3 (-0.86) and T_3S_2 (-0.55) also exhibit significant negative correlations, suggesting that these signals act differently from template T_3 . The weak or nearly neutral correlation (0.3) between T_1 and S_1 indicates that there is no alignment at all. In general, this heat map successfully illustrates strong positive matches (red regions) and strong negative mismatches (blue regions), allowing us to fully investigate the similarity and inversivity of the relationships between particular templates and signals.

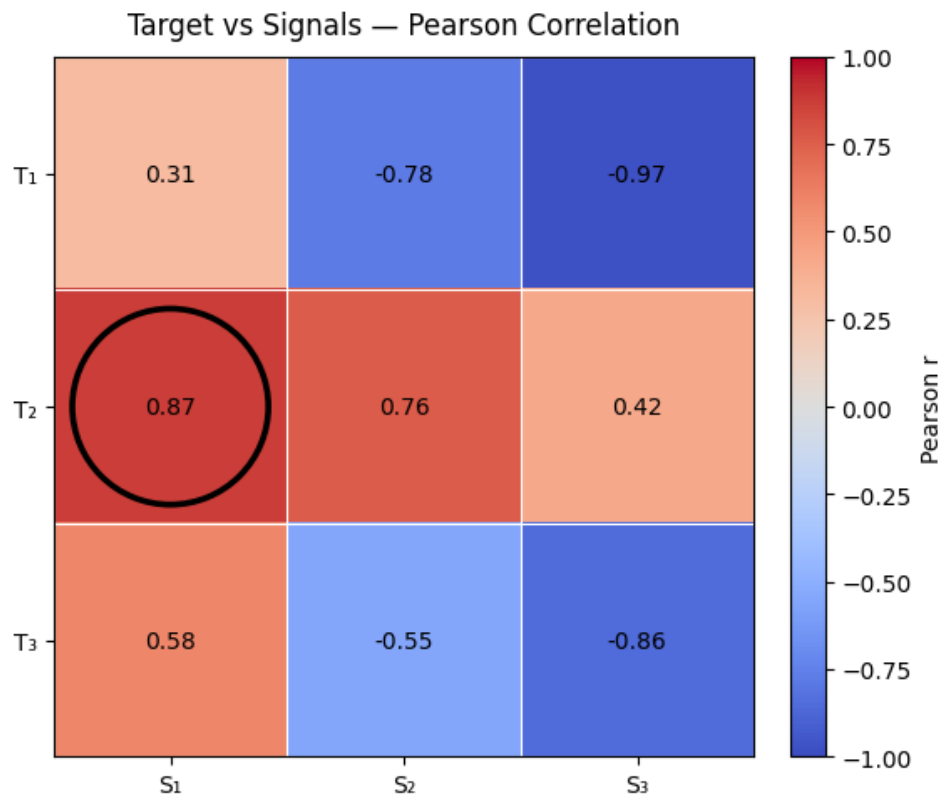


Figure 3

A red-yellow-green color map that smoothly shifts from red (low correlation, 0.000) and yellow (moderate, 0.500) to green (high correlation, 1.000) is used in Fig.4 to generate 2D Normalized Pearson Correlation Heat maps that illustrate the relationships between signals ($S_1 - S_3$) and templates ($T_1 - T_3$). The brilliant green (2.3) indicates a highly significant positive correlation, whilst the deep red (0.001) reveals hardly no association at all. The circle at $T_2 - S_1$ (0.936), which likewise shows perfect alignment and reliability, has the strongest significant link. T_2S_2 (0.882), which is also a significant and good positive association, comes after it. T_3S_1 (0.792) and T_2S_3 (0.709), which show a strong but marginally weaker signal-template correlation, may also show other close connections. On the other hand, the correlations between T_1 and S_3 (0.014) and T_3 and S_3 (0.072) are practically insignificant, suggesting that these signals don't provide any insight into the role of templates T_1 and T_3 in that dimension. Because of their weak correlations, T_1S_2 (0.109) and T_3S_2 (0.223) show low dependability. When compared to stronger couples, the modest T_1S_1 correlation (0.655) shows fair but not leading alignment.

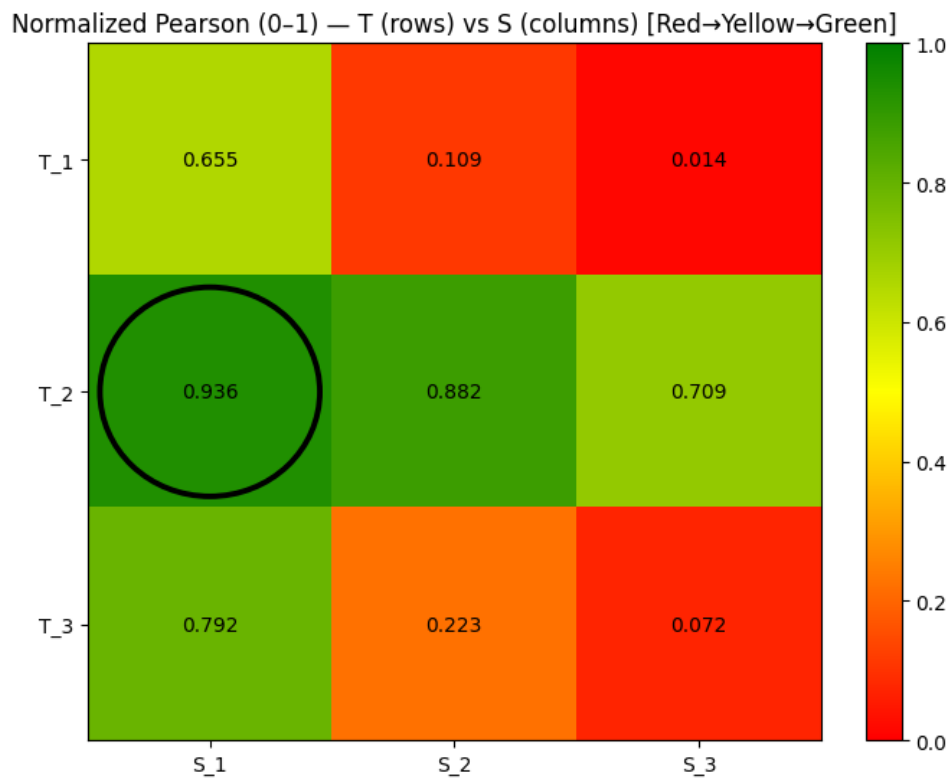


Figure 4

The Cot SM's grouped bar chart between targets ($T_1 - T_3$) and signals ($S_1 - S_3$) is displayed in Fig.5. The distinct contribution of each target is represented by three colored bars, which are blue S_1 , orange S_2 , and green S_3 . The strongest connection between any two sites is seen between T_1 and T_2 , where the maximum annotation value of 0.6653 (highlighted in red) is found. S_1 (0.4913) is reasonably mild at T_1 , but S_2 (0.6653) and S_3 (0.5785) are relatively high. This would suggest that, with a respectable contribution from S_3 , signal S_2 has the biggest influence on target T_1 . S_1 (0.5287) makes the largest contribution in the case of T_2 , whereas S_2 (0.4937) comes in second with a marginally lower value, indicating weaker alignment. Although S_2 (0.4604) is slightly higher than S_3 (0.4221) and S_1 (0.4110), the three signals are significantly closer at T_3 . It implies that while the signals' aggregate contribution to this goal is still modest, it is becoming increasingly reliable. S_2 , which continuously circles the top of each target and reaches the global maximum (0.6653 at T_1), is typically the strongest signal. S_3 , on the other hand, fluctuates, peaking at T_1 and falling at T_2 . S_1 has an average overall performance, doing well at T_2 but poorly elsewhere.

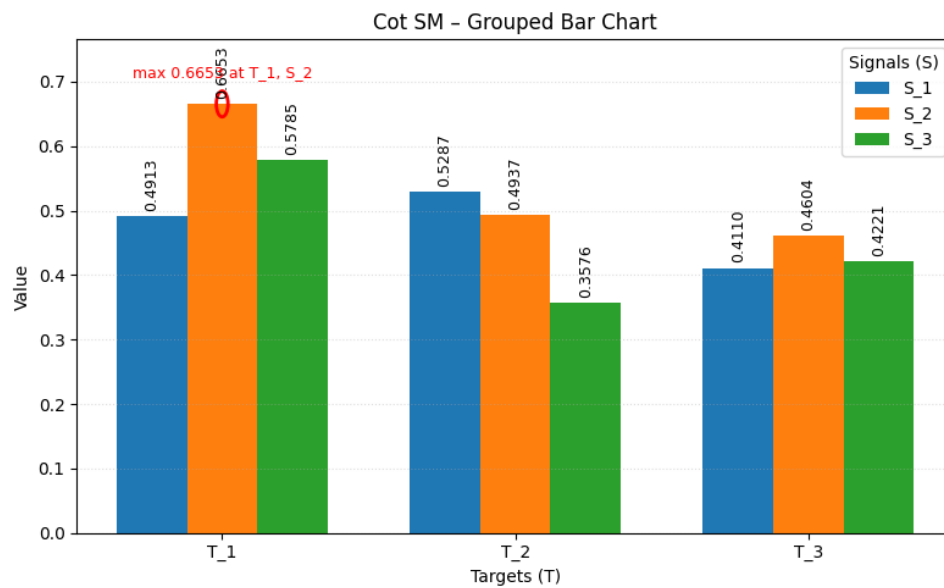


Figure 5

The 3D grouped bar chart in Fig.6 shows the Cot SM values between groups of signals ($S_1 - S_3$) and targets ($T_1 - T_3$). The highest value is indicated by the red highlight. Each bar's height indicates the value that was measured, while the annotation numbers show the precise magnitudes. The red indicates that the maximum value of 0.6653 is obtained at $T_1 S_2$. For the data, this is the optimal signal target alignment. As a result, even though they are much below the maximum value, the contributions of S_3 at T_1 (0.5785) and S_1 at T_2 (0.5287) are still quite considerable. With S_1 being moderate (0.4913), S_3 being considerable (0.5785), and S_2 being dominating (0.6653), the distribution is scattered at T_1 . S_1 contributes the most (0.5287), followed by S_2 (0.4937), and S_3 (0.3576), which contributes the least. At T_3 , values are more evenly distributed, and the closer proximity of S_2 (0.4604), S_3 (0.4221), and S_1 (0.4110) indicates balanced but weaker correlations. With the highest value and overall maximum for each target, S_2 is the strongest signal overall. S_3 behaves differently; it is strong at T_1 and weak at T_2 . Since primacy is only gained at T_2 and lost to S_2 , S_1 is a slow and intermediate reaction.

Cot SM - 3D Bar Chart (max highlighted)

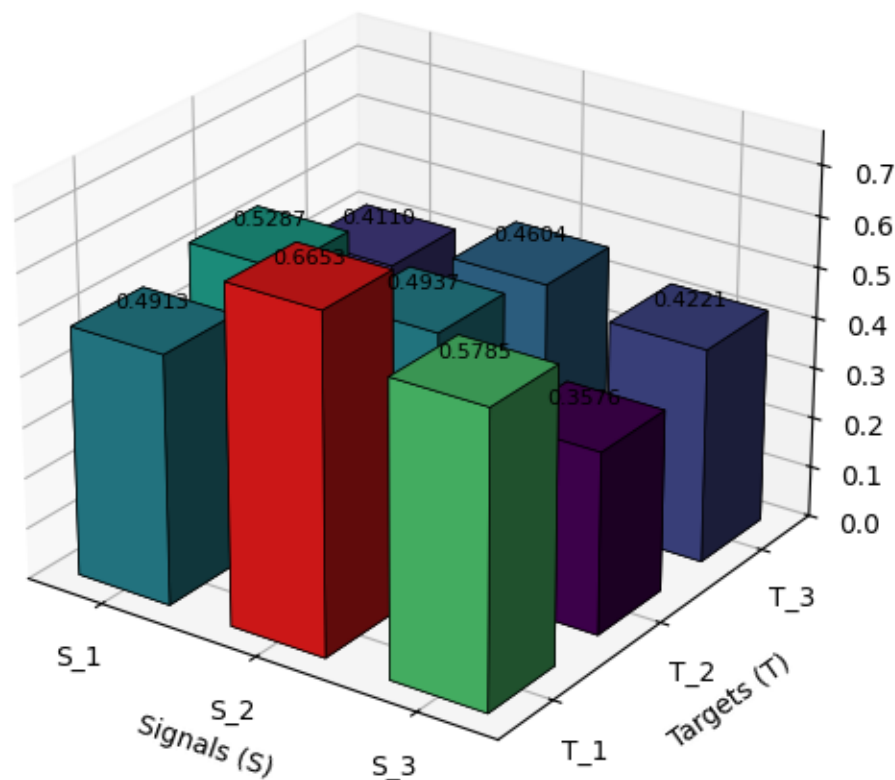


Figure 6

The Cot SM values of the signals ($S_1 - S_2$) and targets ($T_1 - T_2$) are displayed on the 3D surface map of Fig.7. Between the measured places, the surface itself fades consistently, and the color shading (from purple = 0.35 to green 0.55 to yellow 0.66) shows how big the values are. With a maximum of 0.6653 at T_1S_2 , the highest point on the surface is likewise light red. The surface rises sharply at T_1 , with S_2 (0.6653) having the highest ridge and S_3 (0.5785) being higher than S_1 (0.4913). This suggests that S_2 has a stronger and more overwhelming effect on this target than S_1 , even when S_3 complements S_2 . At T_2 , the ground flattens out as it approaches the lower level. S_2 (0.4937), in particular S_3 (0.3576), are buried in lesser contributions that produce a surface dip, while S_1 (0.5287) is the local maximum in this case. On T_3 , the surface is smoother and more consistent, although S_2 (0.4604), S_3 (0.4221), and S_1 (0.4110) appear to be a more or less flat plateau. This demonstrates that the inputs of the signals are equal but comparatively lesser. S_2 is the main signal with the global peak, according to the surface, and it is highly prevalent in all targets when viewed holistically. S_3 is highly variable, favoring T_1 and collapsing at T_2 . S_1 is medium and unstable, peaking around T_2 , however it is less than S_2 .

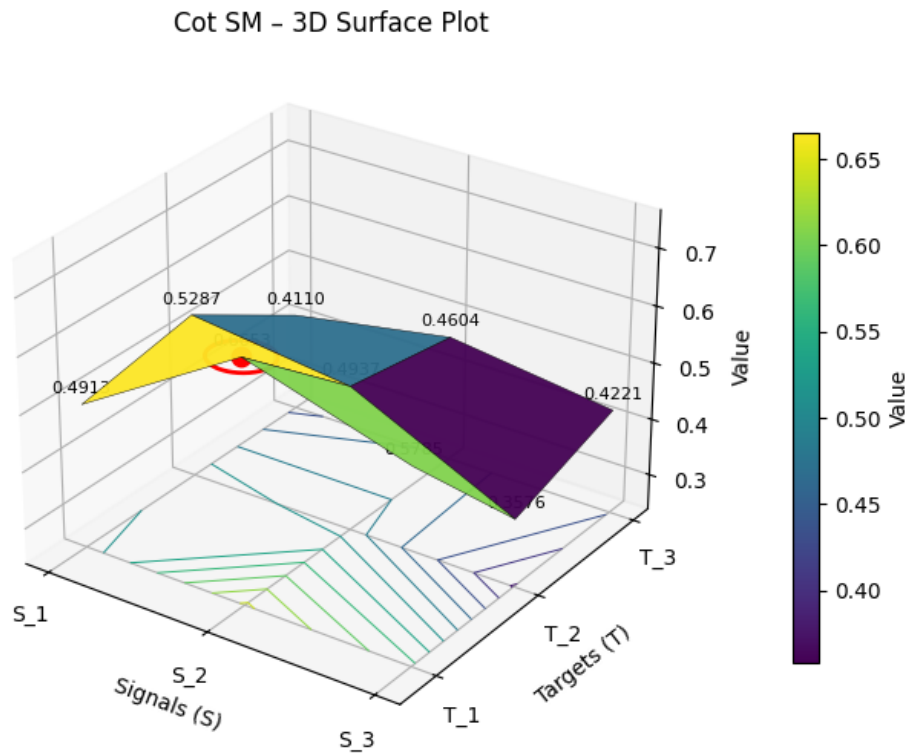


Figure 7

In Fig.8, the 3D surface plot displays the values of the Cot SM on the global scale of $[0-1]$, allowing for instantaneous comparison of the relative intensities of each signal-target combination. The strongest color is bright yellow (1.0), followed by green (0.5), which is in the middle, and deep purple (0.0), which is the weakest. The maximum point of 1.000 at T_1S_2 , the highest point of the normalized surface, is shown in red. S_2 (1.000) dominates all other pairings, and the surface increases dramatically at T_0 . S_3 's contribution (0.556) is also significant, even if S_1 's (0.435) is small. T_1 is currently the most influential target as a result of S_2 's significant influence. The surface sharply declines at T_2 . Despite being the local maximum, S_1 (0.5287 raw, 0.442 normalized) is still far lower than the global maximum. The small contributions of S_3 (0.000) and S_2 (0.174) create a significant dip. At T_3 , the surface flattens out onto a little plateau. The values of S_2 (0.334), S_3 (0.210), and S_1 (about 0.334), which are concentrated at the low end, show equilateral but marginally significant relationships. In general, T_1S_2 performs better than any other combination and is dominant in normalization. S_2 , the strongest signal in the planet, is concentrated at T_1 before suddenly decreasing. S_1 is the most symmetrical since its contributions at T_2 and T_3 are balanced. S_3 is significant at T_1 but insignificant at T_2 because of its great volatility.

Cot SM – 3D Surface Plot (normalized: global)

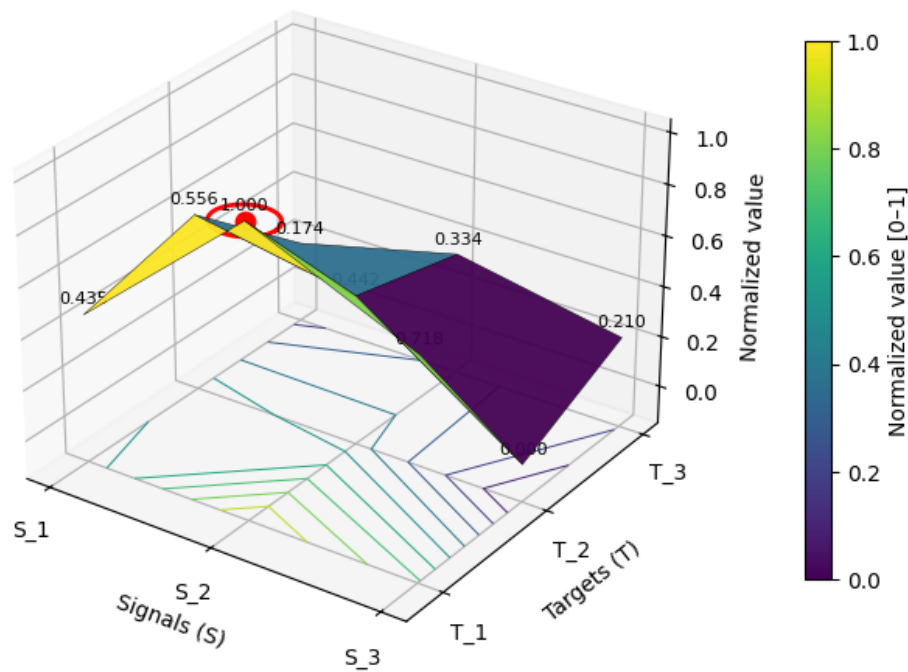


Figure 8

The spline-smoothed functional curves in Fig.9 show the similarity trends (Cot SM) of $T_1 - T_3$ over $S_1 - S_3$. To uncover the underlying functional patterns, the curves are used to interpolate the observed points. In the case of T_1 (blue curve), the similarity between S_1 (0.491) and the global maximum at S_2 (0.665) increases dramatically before progressively decreasing to S_3 (0.579). Consequently, T_1 (the target) becomes the best-performing target and S_2 (the target signal) the dominant target. S_1 (0.529) has medium values for T_2 (the green curve), followed by S_2 (0.494) with marginal values and S_3 (0.358) with sharp values. This downward trend indicates a reduced correlation between the signals, with a tiny S_1 support. In the case of T_3 (orange curve), when S_1 (0.411) peaks at S_2 (0.460) and ends with S_3 (0.422), the similarity is typically the lowest and most balanced. This points to a small yet stable alignment without any noticeable peaks. In conclusion, T_2 exhibits obvious decay, T_3 is weak but stable, and T_1 is dominant because of its high peak at S_2 .

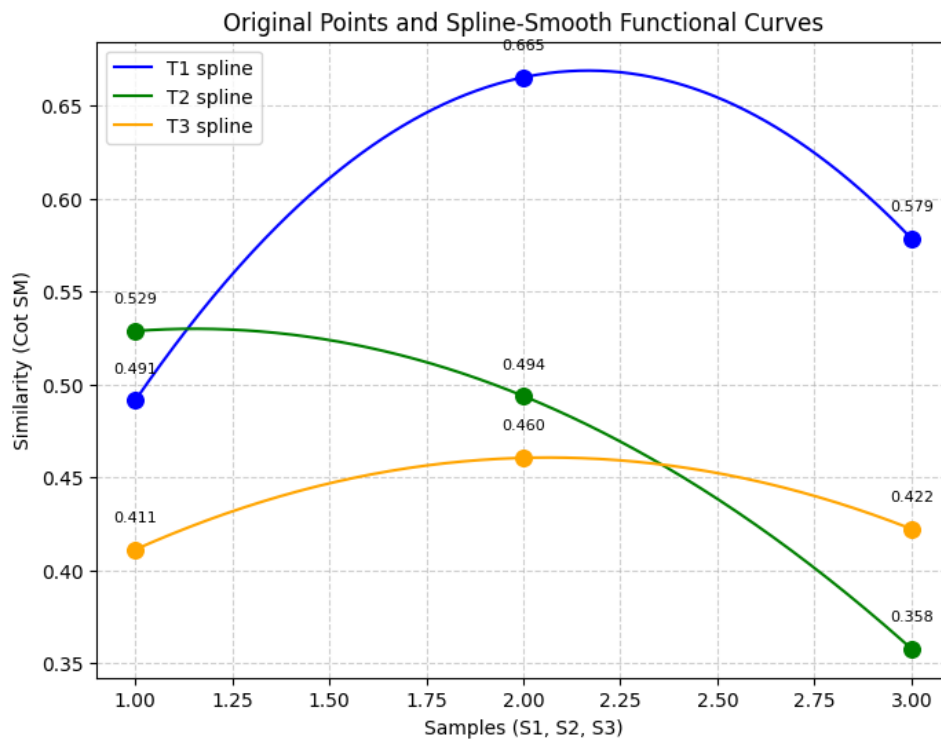


Figure 9

7. Aspect-Method Hybrid Analysis of Signal-Template

In this part, the relationships between signals $S_1 - S_3$ and templates $T_1 - T_3$ are examined using a combination of aspect-based reasoning and method-based validation. In order to identify the most conclusive signal-template alignments, the aspect-based analysis, on the one hand, highlights the current similarity associations and classifies them based on their strength level. Rather, the method-based study demonstrates how these relationships are shown, normalized, and supported in a range of visualization tools, including spline-smoothed curves, Heatmaps, and 3D surfaces. When combined, these complementary viewpoints can ensure both a high level of statistical accuracy and a clear visual representation for interpreting alignment patterns.

7.1. Aspect-based Analysis

The correlations between signals and templates can be organized into three strength tiers: High/Strong (0.58 -0.66): $S_2 - T_1$ (0.6653) is the most reliable match, appearing in several figures with the highest worldwide abundance, making it the most authoritative signal-template match. $S_3 - T_1$ (0.5785) and $S_1 - T_2$ (0.5287) are the second and third weakly stronger and validated commonalities. Associations that are moderate (0.46 -0.49): In the intermediate range are the $S_2 - T_2$ (0.4937) and $S_2 - T_3$ -associations (0.4604). These results show moderate dependability, which gives categorization tasks secondary reinforcement even when they are not definitive. associations that are weak (less than 0.42): The weak zone has the lower values $S_1 - T_3$ (0.4110) and $S_3 - T_3$ (0.4221). The weakest alignment is indicated by $S_3 T_2$, which has the lowest correlation (0.3576). Without further validation, it is impossible to rely on such relationships to yield legitimate matches. Signal S_2 consistently dominates the aspect-based analysis, closely paired with T_1 and having a weak correlation with other templates. In contrast to signal S_1 , which has an intermediate effect, particularly with T_2 , signal S_3 has a varied effect, being quite powerful with T_1 but modest otherwise.

7.2. Method-based Analysis

The method-based study demonstrates how several visualization techniques are used to make these relationships interpretable:

The use of color gradients makes strong matches immediately visible with the heatmaps (Figs.1-4). S_2T_1 (yellow zone) is immediately conspicuous due to the Viridis colormap in Fig.1 and 2 showing absolute and normalized Cotangent Similarity (Cot SM) values. The Pearson correlation maps (Figs. 3-4) are subtle by highlighting both negative and positive alignments (e.g., $T_1 - S_3 = +0.97$ vs. $T_2 - S_1 = +0.87$). Grouped Bar Charts (Figs.5-6) provide proportional influence because they quantify the contributions per signal. An example is, S_1 weaker (0.4913) and S_2 dominant (0.6653) at T_1 , which supports the relative hierarchy that Heatmaps merely suggests. Similarities are depicted as a landscape in 3D Surface Plots (Figs.7-8): the peaks ($T_1 - S_2$) and troughs (T_3 alignments) provide a topographical perspective.

8. Four- Dimensional Evaluation of Analytical Techniques

Four analytical dimensions-visibility, associativity, dynamicity, and scalability-are employed to thoroughly examine the methodologies. These provide a measure of how well each visualization captures, conveys, and extrapolates the interactions between the template and the signal.

Table 4: Factor-Based Comparison of Analytical Techniques

Factors	Heat Map	Grouped Bar	3D Bar	3D Surface	Normalized Surface	Spline-Smoothed Curves
Visibility	Strong (clear gradients)	Strong (explicit values)	Strong (height + color)	Strong (surface peaks)	Very Strong (normalized clarity)	Strong (trend-focused)
Associativity	Strong ($S_2 - T_1$ highlighted)	Strong (signal hierarchy)	Strong (local dominance visible)	Very Strong (peaks vs. troughs)	Very Strong (row-wise contrast)	Strong (trend associations)
Dynamicity	Medium (static gradients)	Medium (comparative only)	Medium (peaks highlighted)	Strong (surface shifts)	Very Strong (normalized extremes)	Very Strong (peaks/troughs trends)
Scalability	Medium-Strong (works for small/medium grids)	Strong (clear for 3-10 signals)	Medium (clutter risk in large sets)	Medium (limited to low dimensions)	Very Strong (scales 0-1 globally)	Strong (curves generalize well)

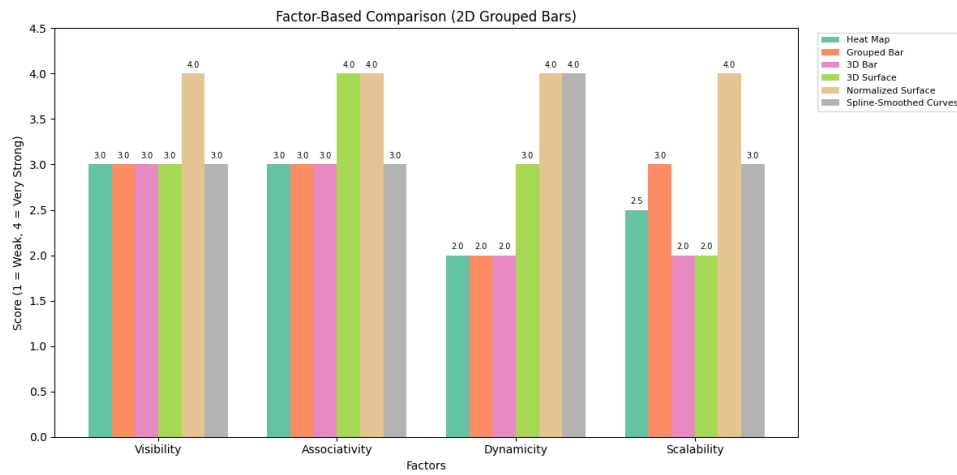


Figure 10

Factor-Based Comparison (3D Bars)

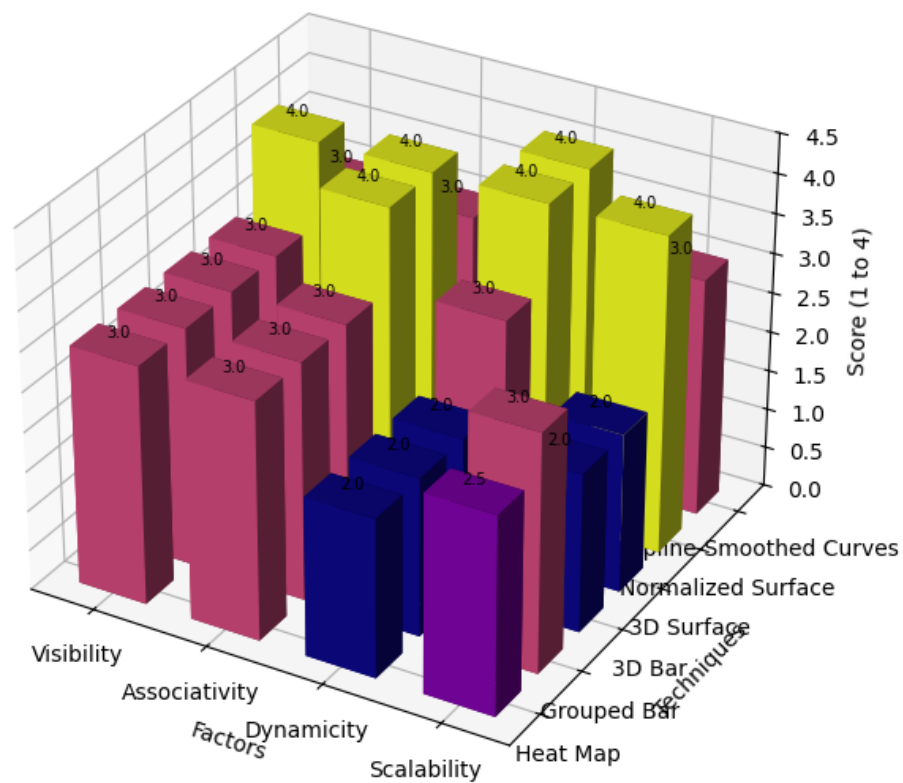


Figure 11

9. Conclusion

The topology of CNS sets (CNSS) and complex single-valued neutrosophic special sets is presented in this paper, creating a robust and novel theoretical framework. By characterizing basic set-theoretic functions and more intricate topological restrictions such as interior and closure, we established a formal mathematical basis to handle complex, ambiguous, and imprecise information. Its usefulness was clearly demonstrated by using this method to a signal-template

alignment challenge. We were able to obtain these systematic analysis results, which displayed results that were simple to comprehend, by using a multidimensional visualization technique and the Cotangent Similarity Measure. With a high-confidence similarity score of 0.6653, $S_2 - T_1$ was repeatedly recognized by the structure as the best match, a global maximum. Additionally, it enabled a thorough description of the signals, showing that S_2 had the highest overall influence and that S_1 and S_3 had higher target-specific values. This study shows the practical utility of topology as a tool for data analysis and pattern discovery, as well as the theoretical validity of the CNSS topology.

10. Limitations

Despite the good results, the current study has certain limitations. The size of the analysis (three signals and three templates) was relatively small in the first case, and this was analytically verified. It has not been confirmed whether the framework is scalable and computationally efficient when working with large, high-dimensional datasets. Second, the model's performance depends on the similarity metric that is selected (in this example, Cot SM), and it has not been investigated how the model behaves in topological space when using different distance or similarity metrics. Thirdly, the method was limited to a single domain (signal alignment) and has not yet been demonstrated to be applicable to any other domain (e.g., medical diagnostics or financial predictions). Finally, due to domain expertise, automated algorithms may struggle to identify the best parameter set to use the neutrosophic soft sets in a particular scenario.

11. Future work

Some interesting directions for future research are based on the model and the findings presented here. The second phase would be scaling to large amounts of real-world data to fully test the computing performance and stability of the application. We will also study other similarity and distance metrics in the CNSS topological space to determine the optimal measures that may be applied to different kinds of problems. One particularly interesting direction to pursue is turning this framework into a comprehensive classification or decision-making algorithm that might be applied to the development of a Complex Neutrosophic Soft Classifier. Additionally, this paradigm is probably going to be applied in the future to other, more sophisticated fields like complex network analysis, multi-sensor data fusion, and image processing. Finally, to make the provided framework more user-friendly, it would be helpful to look into the possibility of automating the settings of the neutrosophic sets.

Acknowledgements

The authors extend their appreciation to Prince Sattam bin Abdulaziz University for funding this research work through the project number (PSAU/2025/01/34111).

Author Contribution: All authors read and approved the final manuscript.

Funding: Prince Sattam bin Abdulaziz University through the project number (PSAU/2025/01/34111).

Conflicts of Interest: The authors declare that they have no conflict of interest to report regarding the present study.

References

- [1] L. A. Zadeh, Fuzzy sets, *Information and Control*, vol. 8, pp. 338-353, 1965.
- [2] D. Ramot, R. Milo, M. Friedman, A. Kandel, Complex fuzzy sets. *IEEE Trans. Fuzzy Syst.* vol. 10, pp. 171-186, 2002.

- [3] A. Alkouri, and A. Salleh, Complex intuitionistic fuzzy sets, in Proceedings of the International Conference on Fundamental and Applied Sciences (ICFAS 12), vol. 1482 of *AIP Conference Proceedings*, pp. 464-470, 2012.
- [4] M. Ali, F. Smarandache, Complex neutrosophic set. *Neural Comput. Appl.* vol. 28, pp. 1817-1834, 2017.
- [5] M. Ali, L. Q. Dat, F. Smarandache, Interval complex neutrosophic set: Formulation and applications in decision-making. *Int. J. Fuzzy Syst.* vol. 20, pp. 986-999, 2018.
- [6] Y. Al-Qudah, N. Hassan, Operations on complex multi-fuzzy sets. *Journal of Intelligent and Fuzzy Systems*, vol. 33(3), pp. 1527-1540, 2017.
- [7] H. Garg, D. Rani, Complex interval-valued intuitionistic fuzzy sets and their aggregation operators. *Fundamenta Informaticae*, vol. 164(1), pp. 61-101, 2019.
- [8] H. Garg, T. Mahmood, A. U. Rehman, Ali, Z. CHFS: Complex hesitant fuzzy sets their applications to decision making with different and innovative distance measures. *CAAI Transactions on Intelligence Technology*, vol. 6(1), pp. 93-122, 2021.
- [9] P. K. Singh, Complex vague set based concept lattice. *Chaos, Solitons and Fractals*, vol. 96, pp. 145-153, 2017.
- [10] S. RaBroumi, A. Bakali, M. Talea, F. Smarandache, P. K. Singh, V. Uluay, M. Khan, Bipolar complex neutrosophic sets and its application in decision making problem. In *Fuzzy Multi-criteria Decision-Making Using Neutrosophic Sets*; Springer: Cham, pp. 677-710, 2019.
- [11] S. G. Quek, S. Broumi, G. Selvachandran, A. Bakali, M. Talea, F. Smarandache, Some results on the graph theory for complex neutrosophic sets. *Symmetry*, vol. 10(6), art. 190, 2018.
- [12] A. Al-Quran, S. Alkhazaleh, Relations between the complex neutrosophic sets with their applications in decision making. *Axioms*, vol. 7(3), art. 64, 2018.
- [13] L. Q. Dat, N. T. Thong, M. Ali, F. Smarandache, M. Abdel-Basset, H. V. Long, Linguistic approaches to interval complex neutrosophic sets in decision making. *IEEE Access*, vol. 7, pp. 38902-38917, 2019.
- [14] D. Molodtsov, Soft set theory-first results. *Comput. Math. Appl.* vol. 37, pp. 19-31, 1999.
- [15] P.K. Maji, R. Biswas, A. R. Roy, Fuzzy soft sets. *J. Fuzzy Math.* vol. 9, pp. 589-602, 2001.
- [16] P.K. Maji, R. Biswas, A.R. Roy, Intuitionistic fuzzy soft sets. *J. Fuzzy Math.* vol. 9(3), pp. 677-692, 2001.
- [17] B. Chetia, P. K. Das, An application of interval-valued fuzzy soft. *Int. J. Contemp. Math. Sci.* vol. 5(38), pp. 1887-1894, 2010.
- [18] Y. Jiang, Y. Tang, Q. Chen, H. Liu, J. Tang, Interval-valued intuitionistic fuzzy soft sets and their properties. *Comput. Math. Appl.* vol. 60(3), pp. 906-918, 2010.
- [19] P.K. Maji, Neutrosophic soft set. *Ann. Fuzzy Math. Inform.* vol. 5, pp. 157-168, 2013.
- [20] I. Deli and S. Broumi, Neutrosophic soft relations and some properties, *Annals of Fuzzy Mathematics and Informatics*, vol. 9(1), pp. 169-182, 2015.
- [21] T.Bera and N. K. Mahapatra, Introduction to neutrosophic soft topological space, *Opsearch*, vol. 54(4), pp. 841-867, 2017.
- [22] I. Deli, Interval-valued neutrosophic soft sets and its decision making. *Int. J. Mach. Learn. Cyber.* vol. 8(2), pp. 665-676, 2017.
- [23] M. Abu Qamar, N. Hassan, An approach toward a Q-neutrosophic soft set and its application in decision making. *Symmetry*, vol. 11(2), art. 139, 2019.
- [24] M. Abu Qamar, A.G. Ahmad, N. Hassan, On Q-neutrosophic soft fields. *Neutrosophic Sets Syst.* vol. 32, pp. 80-93, 2020.
- [25] P. Thirunavukarasu, R. Suresh, V. Ashokkumar, Theory of complex fuzzy soft set and its applications. *Int. J. Innov. Res. Sci. Technol.* vol. 3(10), pp. 13-18, 2017.
- [26] G. Selvachandran, P. K. Singh, Interval-valued complex fuzzy soft set and its application. *Int. J. Uncertain. Quantif.* vol. 8(2), 2018.

- [27] T. Fujita. The Hyperfuzzy VIKOR and Hyperfuzzy DEMATEL Methods for Multi-Criteria Decision-Making. *Spectrum of Decision Making and Applications*, vol. 3(1), pp. 292-315, 2025.
- [28] R. Gul. An Extension of VIKOR Approach for MCDM Using Bipolar Fuzzy Preference d-Covering Based Bipolar Fuzzy Rough Set Model. *Spectrum of Operational Research*, vol. 2(1), pp. 72-91, 2025.
- [29] M. E. M. Abdalla, A. Uzair, A. Ishtiaq, M. Tahir., & M. Kamran. Algebraic Structures and Practical Implications of Interval-Valued Fermatean Neutrosophic Super Hyper Soft Sets in Healthcare. *Spectrum of Operational Research*, vol. 2(1), pp. 199-218.
- [30] T. Kumar, R. K. Bajaj, On complex intuitionistic fuzzy soft sets with distance measures and entropies. *J. Math.* 2014.
- [31] G. Selvachandran, P. K. Maji, I. E. Abed, A. R. Salleh, Complex vague soft sets and its distance measures. *J. Intell. Fuzzy Syst.* vol. 31(1), pp. 55-68, 2016.
- [32] S. Broumi, A. Bakali, F. Smarandache, M. Talea, M. Ali, G. Selvachandran, Complex neutrosophic soft set. In Proceedings of the FUZZ-IEEE Conference on *Fuzzy Systems*, 2017.
- [33] Z. Ali, T. Mahmood, M. Aslam, R. Chinram, Another view of complex intuitionistic fuzzy soft sets based on prioritized aggregation operators and their applications to multiattribute decision making. *Mathematics*, vol. 9(16), art. 1922, 2021.
- [34] A. Al-Quran, N. Hassan. The CNS expert set and its application in decision making. *J. Intell. Fuzzy Syst.* vol. 34, 569-582, 2018.
- [35] Y. Al-Qudah, N. Hassan, Complex multi-fuzzy soft expert set and its application. *Int. J. Math. Comput. Sci.*, vol. 14(1), pp. 149-176, 2019.
- [36] Y. Al-Qudah, M. Hassan, N. Hassan, Fuzzy parameterized complex multi-fuzzy soft expert set theory and its application in decision-making. *Symmetry* vol. 11(3), art. 358, 2019.
- [37] M. AlAkram, U. Amjad, J. C. R. Alcantud and G. Santos-Garcia, Complex Fermatean Fuzzy N-Soft Sets: A New Hybrid Model with Applications. *J. Ambient Intell. Humaniz. Comput.*, vol. 13, pp. 1-34, 2022.
- [38] A. Al-Quran, S. Alkhazaleh, L. Abdullah, Complex Bipolar-Valued Neutrosophic Soft Set and its Decision Making Method. *Neutrosophic Sets Syst.* vol. 47, pp. 105-116, 2021.
- [39] M. Akram, M. Shabir, A. Ashraf, Complex neutrosophic N-soft sets: A new model with applications. *Neutrosophic Sets Syst.* vol. 42, pp. 278-301, 2021.
- [40] A. Al-Quran, N. Hassan, The CNS expert relation and its multiple attribute decision-making method. *Entropy*, vol. 20, art. 101, 2018.
- [41] F. Al-Sharqi, A. Al-Quran, A. G. Ahmad, S. Broumi, Interval-valued CNS set and its applications in decision-making. *Neutrosophic Sets Syst.* vol. 40, pp. 149-168, 2021.
- [42] F. Al-Sharqi, A. Al-Quran, A. G. Ahmad, Interval-Valued Neutrosophic Soft Expert Set from Real Space to Complex Space. *Comput. Model. Eng. Sci.* vol. 132(1), pp. 267-293, 2022.
- [43] F. Al-Sharqi, A. Al-Quran, A. G. Ahmad, Interval CNS relations and their application in decision-making. *J. Intell. Fuzzy Syst.* vol. 43(1), pp. 745-771, 2022.
- [44] M. Saqlain, N. Jafar, S. Moin, M. Saeed, S. Broumi, Single and multi-valued neutrosophic hypersoft set and tangent similarity measure of single valued neutrosophic hypersoft sets. *Neutrosophic Sets Syst.* vol. 32(1), pp. 317-329, 2022.
- [45] S. Begam , G. Selvachandran, T. T. Ngan, R. Sharma, Similarity measure of lattice ordered multi-fuzzy soft sets based on set theoretic approach and its application in decision making. *Mathematics*, vol. 8(8), art. 1255, 2020.
- [46] R. M. Zulqarnain, I. Siddique, M. Asif, S. Ahmad, S. Broumi, S. Ayaz, Similarity Measure for m-Polar Interval Valued Neutrosophic Soft Set with Application for Medical Diagnoses. *Neutrosophic Sets Syst.* vol. 47(1), pp. 147-164, 2021.
- [47] D. Liu, G. Liu, Z. Liu, Some similarity measures of neutrosophic sets based on the Eu-

- clidean distance and their application in medical diagnosis. *Comput. Math. Methods Med.*, art. 9, 2018.
- [48] K. Ullah, T. Mahmood, N. Jan, Similarity measures for T-spherical fuzzy sets with applications in pattern recognition. *Symmetry*, vol. 10(6), art. 193, 2018.
 - [49] A. U. Rahman, M. Saeed, H. A. E. W. Khalifa, W. A. Afifi, Decision making algorithmic techniques based on aggregation operations and similarity measures of possibility intuitionistic fuzzy hypersoft sets. *AIMS Math.* vol. 7(3), pp. 3866-3895, 2021.
 - [50] S. Broumi, F. Smarandache, Several Similarity Measures of Neutrosophic Sets. *Neutrosophic Sets Syst.* vol. 1, pp. 54-62, 2013.
 - [51] J. Ye, Similarity measures between interval neutrosophic sets and their applications in multi criteria decision-making. *J. Intell. Fuzzy Syst.* vol. 26(1), pp. 165-172, 2014.
 - [52] A. Mukherjee, S. Sarkar, Several similarity measures of interval valued neutrosophic soft sets and their application in pattern recognition problems. *Neutrosophic Sets Syst.* vol. 6, pp. 55-61, 2014.
 - [53] M. Abu Qamar, N. Hassan, Entropy, measures of distance and similarity of Q-neutrosophic soft sets and some applications. *Entropy*, vol. 20(9), art. 672, 2018.
 - [54] Y. Al-Qudah, N. Hassan, Complex multi-fuzzy soft set: Its entropy and similarity measure. *IEEE Access*, vol. 6, pp. 65002-65017, 2018.
 - [55] G. Selvachandran, H. Garg, M. H. Alaroud, A. R. Salleh, Similarity measure of complex vague soft sets and its application to pattern recognition. *Int. J. Fuzzy Syst.*, vol. 20(6), pp. 1901-1914, 2018.
 - [56] D. Xu, X. Cui, L. Peng, H. Xian, Distance measures between interval complex neutrosophic sets and their applications in multi-criteria group decision making. *AIMS Math.* vol. 5(6), pp. 5700-5715, 2020.
 - [57] F. Smarandache, Neutrosophic set, a generalisation of the intuitionistic fuzzy sets. *Int. J. Pure Appl. Math.* vol. 24, pp. 287-297, 2005.
 - [58] F. Smarandache, Neutrosophy: Neutrosophic Probability, Set and Logic; *American Research Press: Rehoboth, IL, USA*, 1998.
 - [59] H. Wang, P. Madiraju, Y. Zhang, R. Sunderraman, Interval Neutrosophic Sets. *arXiv* 2004, math/0409113.
 - [60] A. Khalid, M. Abbas, Distance measures and operations in intuitionistic and interval-valued intuitionistic fuzzy soft set theory. *Int. J. Fuzzy Syst.*, vol. 17(3), pp. 490-497, 2015.
 - [61] F. Smarandache, Extension of Soft Set to HyperSoft Set, and then to Plithogenic Hyper-soft Set. *Neutrosophic Sets Syst.* vol. 22, pp. 168-170, 2018.
 - [62] M. M. Abed, N. Hassan, F. Al-Sharqi, On Neutrosophic Multiplication Module. *Neutrosophic Sets Syst.* vol. 47, pp. 198-208, 2022.
 - [63] N. A. Alhaleem, A.G. Ahmad, Intuitionistic Anti Fuzzy Normal Subrings over Normed Rings. *Sains Malays.* vol. 51(2), pp. 609-618, 2022.
 - [64] F. G. Al-Sharqi, M. M. Abed, A. A. Mhassin, On Polish Groups and their Applications. *J. Eng. Appl. Sci.* vol. 13(18), pp. 7533-7536, 2018.
 - [65] M. M. Abed, F. Al-Sharqi, S. H. Zail, A Certain Conditions on Some Rings Give P.P. Ring. *J. Phys. Conf. Ser.* vol. 1818, art. 012068, 2021.
 - [66] M. M. Abed, F. G. Al-Sharqi, Classical Artinian module and related topics. *J. Phys. Conf. Ser.* vol. 1003, art. 012065, 2018.
 - [67] M. M. Abed, F. G. Al-Sharqi, A. A. Mhassin, Study fractional ideals over some domains. *AIP Conf. Proc.* vol. 2138, art. 030001, 2019.
 - [68] M. M. Abed, A. F. Al-Jumaili, F. G. Al-sharqi, Some mathematical structures in a topological group. *J. Algebra Appl. Math.* vol. 16(2), pp. 99-117, 2018.
 - [69] M. M. Abed, F. G. Al-Sharqi, Classical Artinian module and related topics. *J. Phys. Conf. Ser.* vol. 1003, art. 012065, 2018.

- [70] A. F. Al-Jumaili, M.M. Abed, F. Al-Sharqi, Other new types of Mappings with Strongly Closed Graphs in Topological spaces via $e - \theta$ and $\delta - \beta - \theta$ open sets. *J. Phys. Conf. Ser.*, vol. 1234, art. 012101, 2019.
- [71] S. A. El-Sheikh, & A. M. Abd El-Latif. Decompositions of some types of supra soft sets and soft continuity. *Int. J. Math. Trends Technol.*, vol. 9(1), pp. 37-56, 2014.
- [72] A. M. Abd El-Latif, & R. A. Hosny. Supra open soft sets and associated soft separation axioms. *Int. J. Adv. Math.*, vol. 6, pp. 68-81, 2017.
- [73] A. M. Abd El-Latif. Soft supra strongly generalized closed sets. *J. Intell. Fuzzy Systems*, vol. 31(3), pp. 1311-1317, 2016.
- [74] A. M. Abd El-Latif, & R. A. Hosny. Soft supra extra strongly generalized closed sets. *An. Univ. Oradea Fasc. Mat.*, vol. 24(1), pp. 103-112, 2017.
- [75] A. M. Abd El-Latif, & R. A. Hosny. Supra soft separation axioms and supra irresoluteness based on supra b-soft sets. *Gazi Univ. J. Sci.*, vol. 29(4), pp. 845-854, 2016.
- [76] A. M. Abd El-Latif. Soft supra strongly *semi** generalized closed sets. *Ann. Fuzzy Math. Inform.*, vol. 13(1), pp. 63-71, 2017.
- [77] A. M. Abd El-Latif, & R. A. Hosny. Supra semi open soft sets and associated soft separation axioms. *Appl. Math. Inf. Sci.*, vol. 10(6), pp. 2207-2215, 2016.
- [78] A. M. Abd El-Latif. Supra soft *b*-connectedness II: Some types of supra soft *b*-connectedness. *Creat. Math. Inform.*, vol. 26(1), pp. 1-8, 2017.
- [79] A. M. Abd El-Latif, & S. Karatas. Soft supra strongly generalized closed sets via soft ideals. *Appl. Math. Inf. Sci. Lett.*, vol. 5(1), pp. 21-26, 2016.
- [80] A. M. Abd El-Latif. On soft supra compactness in supra soft topological spaces. *Tbil. Math. J.*, vol. 11(1), pp. 169-178, 2018.